1 **Changes in microbial composition, diversity, and functionality in the *Amblyomma***

2 ***maculatum* microbiome following infection with *Rickettsia parkeri***

3

4 Abdulsalam Adegoke[1], Deepak Kumar[1], Khemraj Budachetri[1,2], Shahid Karim[1,3]

5

6 [1]School of Biological, Environmental, and Earth Sciences, University of Southern
7 Mississippi, Hattiesburg, MS 39406, USA

8

9 [2]Department of Veterinary Biosciences, The Ohio State University, Columbus, OH
10 43210, USA

11 [3]Center for Molecular and Cellular Biosciences, University of Southern Mississippi,
12 Hattiesburg, MS 39406, USA

13

14

15 *Corresponding author:

16 Shahid.Karim@usm.edu

17

18

19 **Abstract**

20 **Background**

21 Ticks are the primary vectors for emerging and resurging pathogens of public health
22 significance worldwide. Examining tick bacterial composition, diversity, and functionality
23 across developmental stages and tissues is necessary for designing new strategies to
24 control ticks and prevent tick-borne diseases.

25 **Methods**

26 A high-throughput sequencing approach was used to determine the influence of blood
27 meal and *Rickettsia parkeri* infection on changes in *Amblyomma maculatum*
28 microbiome composition, diversity, and functionality across the developmental timeline
29 and in different tissues. Quantitative insight into microbial ecology analysis allowed us to
30 determine microbial population structure, composition, and diversity. A non-metric
31 multidimensional scaling, the sparse correlations for compositional data (SparCC)
32 module, and phylogenetic investigation of communities by reconstruction of unobserved
33 states 2 (PICRUSt2) software were used in the assessment.

34 **Results**

35 The *Amblyomma maculatum* microbiome comprises ten bacterial genera present across
36 tick life cycle stages. Among the top ten bacterial genera (the core tick microbiome),
37 *Rickettsia, Francisella,* and *Candidatus Midichloria* are the key players, with positive
38 interactions within each developmental stage and adult tick organ tested. The bacterial
39 abundances, based on the number of operational taxonomic units (OTUs), increase with
40 blood meal in each stage, helping bacterial floral growth. The growth in bacterial
41 numbers is related to highly abundant energy metabolism orthologs with blood meal,
42 according to functional analysis. Whereas *R. parkeri* had a positive correlation with
43 *Candidatus Midichloria* during the tick life cycle, based on the increased number of
44 OTUs and network analysis, this was due to an increased level of metabolic activity.
45 Interestingly, *R. parkeri* replaces *Francisella,* based on the lower level of OTUs
46 representing *Francisella* in *R. parkeri*-infected ticks (in all stages/organs) and negatively
47 correlated according to network and linear discriminant analysis effect size (LEfSe).

48 **Conclusions**

49 We found that *Rickettsia* and *Francisella* predominate in the core microbiome of the
50 Gulf Coast tick, whereas *Candidatus Midichloria* and *Cutibacterium* levels increase with
51 infection. Network analysis and functional annotation suggest that *R. parkeri* interacts
52 positively with *Candidatus Midichloria* and negatively with *Francisella* and that metabolic
53 profiles are upregulated with blood meal and *R. parkeri* infection. Overall, this is the first
54 study to determine the combinatorial outcome of blood meal and pathogen interaction
55 on microbiome composition over the developmental stages of *Am. maculatum*. This new
56 study expands on our existing knowledge of the *Am. maculatum* microbiome and further
57 highlights the need to investigate pathogen–symbiont interactions between *R. parkeri*
58 and *Francisella* or *Candidatus Midichloria* to facilitate the development of strategies for
59 controlling tick-transmitted diseases.

60

Background

Ticks are obligate hematophagous arthropods that predominantly depend on human and animal host blood for development. Their importance as one of the important vectors of human and animal pathogens is highlighted by the substantial resources channeled towards controlling the several tick-transmitted pathogens. The Gulf Coast tick (*Amblyomma maculatum*) is one of four human-biting ticks in the United States, including also *Amblyomma americanum, Ixodes scapularis,* and *Dermacentor variabilis. Amblyomma maculatum* (*Am. maculatum*) is the most geographically widespread tick species in the southeastern United States (Sonenshine, 2018). It is the competent vector of *Rickettsia parkeri* (*R. parkeri*), a spotted fever group rickettsial (SFGR) pathogen that causes mild infections in the United States (Paddock and Goddard, 2015).

Recent advances in the control of tick and tick-transmitted pathogens have led to the discovery of microbial communities that co-exist alongside pathogens. The functional role of the tick microbiome has only been partly clarified by tick research. Overall, the primary focus of tick microbiome research has been on the microbial profiling of field-collected ticks to understand the basic bacterial profiles/communities present. The tick microbiome is a moving target and investigating its dynamics within the tick vector is a continuing concern (Narasimhan et al., 2015; Bonnet et al., 2017; Greay et al., 2018; Narasimhan et al., 2021). Ticks specialize in an exclusive diet of vertebrate blood and have evolved intimate interactions with beneficial symbionts that provide essential B vitamins and cofactors deficient in the blood diet (Guizzo et al., 2017; Ben-Yousaf et al., 2020; Duron et al., 2017; Bonnet et al., 2017; Duron et al., 2018; Gottlieb et al., 2015; Hunter et al., 2015; Olivieri et al., 2019; Smith et al., 2015), and the nutritional value of essential vitamins provided by the tick microbiome has been related to the reproductive fitness of ticks (Zhong et al., 2007). Immunomodulatory functions have also been associated with microbial communities within the tick and other blood-feeding arthropods, in which certain microbes have been shown to constantly prime the host immune system to continuously produce basal levels of antimicrobial peptides while also directly competing with or facilitating the establishment of different members of these microbial communities (de la Fuente et al., 2017; Fogaca et al., 2021; Boulanger and Wikel, 2021; Bonnet and Pollet, 2021; Budachetri et al., 2018).

96   Several studies have reported on the structure and microbial composition of field-
97   collected and lab-maintained tick populations (Budachetri et al., 2014; Budachetri et al.,
98   2017; Ross et al., 2018; Varela-Stokes et al., 2018; Thapa et al., 2019; Gill et al., 2020;
99   Maldonado-Ruiz et al., 2021; Kumar et al., 2021; Karim et al., 2017; Zhang et al., 2019;
100 Portillo et al., 2019; Adegoke et al., 2020; Guizzo et al., 2020; Rojas-Jaimes et al., 2021).
101 These studies have revealed a variety of factors responsible for the differences among
102 microbial communities between different tick samples, thus contributing extensively to our
103 understanding of how microbial communities residing within the tick contribute to several
104 aspects of tick biology (Ponnusamy et al., 2014; Budachetri et al., 2015; Trout-Fryxell and
105 DeBruyn, 2016; Budachetri et al., 2018; Thapa et al., 2019; Brinkerhoff et al., 2020;
106 Adegoke et al., 2020; Kueneman et al., 2021). However, the structure of *Am. maculatum*
107 microbial communities and how these communities are shaped by blood meal and
108 pathogen interactions have been the focus of only a few studies (Budachetri et al., 2014;
109 Budachetri et al., 2018). Previous microbiome studies of *Am. maculatum* identified unique
110 differences in microbial composition and abundance of specific bacterial genera in field-
111 collected and questing tick tissues (Budachetri et al., 2014). The ability of a tick to serve
112 as a competent vector for any pathogen goes beyond the establishment of the pathogen
113 within the tick tissue but also extends to the facilitation of pathogen transmission at the
114 tick–host interface, which is made possible in part by salivary proteins, in what has been
115 described as saliva-assisted transmission (Nuttal and Labuda, 2008; Šimo et al., 2017;
116 Nuttal, 2019; Karim et al., 2021). Whether the tick salivary microbiome interferes or
117 facilitates pathogen colonization and transmission remains an unanswered question.
118 While a study by Budachetri et al. (2014) reported several *Rickettsia* species in the saliva
119 of *Am. maculatum*, only *R. parkeri* was detected in the salivary glands of *Am. maculatum*.
120 Limited information exists about how microbial community members interact across tick
121 developmental stages and tissues and how these tissues shape or modulate microbial
122 community assemblages during tick physiological changes, such as those following
123 blood-feeding or pathogen interactions. An elegant study by Lejal et al. (2021) identified
124 several positive and negative correlations between members of the field-collected,
125 questing *Ixodes ricinus* microbiome and how some of these interactions are modulated
126 by tick-borne pathogens. It has been established that each tick tissue (organ) undergoes

127 unique responses to specific physiological changes, but it is not known whether these
128 responses also induce changes in the microbial communities residing within these tissues
129 (Franta et al., 2010; Schwarz et al., 2014; Crispell et al., 2016; Kumar et al., 2016;
130 Budachetri et al., 2017; Starck et al., 2018; Tirloni et al., 2020; Kurokawa et al., 2020). In
131 the current study, a high-throughput sequencing approach was utilized to examine
132 microbiome changes throughout the ontogeny of uninfected and pathogen-infected *Am.*
133 *maculatum* ticks. Characterization of unique microbe-microbe interactions at the different
134 tick developmental stages and tissues revealed potential synergistic and antagonistic
135 interactions among the bacterial communities.

136 **Materials and Methods**

137 *Ethics statement*

138 All animal experiments were conducted in strict accordance with the recommendations of
139 the Guide for the Care and Use of Laboratory Animals of the National Institutes of Health,
140 USA. The protocols for the blood-feeding of immature and mature development stages of
141 *Am. maculatum* was approved by the Institutional Animal Care and Use Committee of the
142 University of Southern Mississippi (protocols #15101501.2 and 15011402).

143 *Tick maintenance*

144 *Rickettsia parkeri*-infected and uninfected *A. maculatum* ticks were maintained under
145 laboratory conditions as previously described (Budachetri et al., 2017; 2018). The
146 colonies were established from field-collected adult ticks collected in 2011 from the
147 Mississippi   Sandhill   Crane,   National   Wildlife   Refuge
148 (https://www.fws.gov/refuge/mississippi_sandhill_crane/) using the drag-cloth method.
149 To generate replete adult females, unfed male and female *Am. maculatum* ticks were
150 infested on sheep and allowed to feed to repletion and drop off. Fully engorged female
151 ticks were then allowed to oviposit in individual snap-cap vials with perforated lids
152 protected by breathable mesh cloths to allow for oxygen exchange while preventing their
153 escape. Unfed larvae that emerged from the eggs were infested on golden Syrian
154 hamsters until fully engorged, which were then allowed to molt into nymphs and then
155 reinfested on golden Syrian hamsters. The fully fed nymphs were subsequently allowed

156   to molt into adult male and female ticks. The presence or absence of *R. parkeri* at each

157   developmental stage was confirmed following previously established nested PCR

158   approaches (Budachetri 2014).

Tick life stages and DNA extraction

160   DNA was isolated from freshly laid eggs as well as unfed and partially fed ticks at various

161   developmental stages, including larvae, nymph, male, and female adults. To remove

162   surface contaminants and bacterial carryover, all samples from developmental stages

163   were surface-sterilized using 2% sodium hypochlorite, followed by two 5-minute washes

164   in 70% ethanol and two 5-minute washes in sterile deionized water (Kumar et al., 2021).

165   Tissues were dissected from unfed and partially blood-fed adult females and directly

166   stored in ATL buffer before extracting DNA. Tick dissection was done in a biosafety

167   cabinet while changing blades between dissections. Saliva was collected on ice by

168   endogenous induction of salivation following injection of pilocarpine, as previously

169   described (Ribeiro et al., 2004; Valenzuela et al., 2004). DNA was extracted using the

170   DNeasy Blood and Tissue Kit following the manufacturer's protocol (QIAGEN,

171   Germantown, MD, USA) in a biosafety cabinet to eliminate potential carryover of bacteria

172   between samples. Control samples included a blank control and a mock bacterial sample

173   with a known bacterial population (ZymoBIOMICS™ Microbial Community DNA

174   Standard) as part of the DNA-extraction protocol.

Library preparation for Illumina 16S sequencing

176   Library preparation and indexing were carried out according to Illumina 16S metagenomic

177   sequencing. The V3–V4 region of the 16S rRNA gene was amplified using DNA samples

178   from different life stages and tissues. A two-step PCR amplification was carried out, which

179   included an initial V3–V4 amplification using primers with specific Illumina adapter

180   overhang nucleotide sequences using the following thermocycling conditions: 95°C for 3

181   min; followed by 25 cycles of 95°C for 30 s, 55°C for 30 s, and 72°C for 30 s; and a final

182   extension step of 72 °C for 5 min. The PCR amplicon was briefly purified using AmPure

183   XP beads (Agencourt Bioscience Corporation, Beverly, Massachusetts, USA) following

184   the manufacturer's protocol, and the purified product was eluted in 50 µl of TE buffer

185   (Qiagen cat. no. 19086) and analyzed on a 2% gel to confirm a single DNA band with an

186   estimated amplicon size of 550 bp. The second and most crucial step involved attaching

187   unique indexes, in the form of nucleotide sequences, to the purified V3–V4 PCR product.

188   Commercially available dual indexes (i5 and i7) from the Illumina Nextera index kit V2

189   (Illumina, San Diego, CA) were used for the second (index) PCR. Briefly, a reaction

190   including each of the forward and reverse Nextera index primers, 1X KAPA HiFi HotStart

191   ReadyMix (Kapa Biosystems, Wilmington, MA, USA), and 5 µl of each purified V3–V4

192   amplicon was set up using the following thermocycling conditions: 95°C for 3 min;

193   followed by 8 cycles of 95°C for 30 s, 55°C for 30 s, and 72°C for 30 s; and a final

194   extension step of 72 °C for 5 min. The second (index) PCR product was briefly purified

195   using AmPure XP beads (Agencourt Bioscience Corporation, Beverly, Massachusetts,

196   USA), following the manufacturer's protocol. The purified product was eluted in 25 µl of

197   TE buffer and analyzed on a 2% gel to confirm a single DNA band with an estimated

198   amplicon size of 630 bp. The purified indexed PCR library products were quantified using

199   the KAPA Library Quantification Kit from Roche (cat. no. 07960255001, kit code KK4844),

200   normalized to a concentration of 7 nM, and pooled with 5 µl of each normalized library.

201   Biological replicates from DNA extraction controls, TE buffer, and mock bacterial

202   communities (ZymoBIOMICS™ Microbial Community DNA Standard) were

203   simultaneously processed alongside the tick samples. The purified library was sequenced

204   in a single run of an Illumina MiSeq sequencing instrument using reagent kit v2 (500

205   cycles) with 2 X 250 bp output at the University of Mississippi Medical Centre (UMMC)

206   Genomics Core Facility.

207   *Data processing and analysis*

208   Unless otherwise stated, all preprocessing was done following the video tutorial of the

209   Quantitative Insights into Microbial Ecology (QIIME2) pipeline (Blyen et al., 2019). Briefly,

210   demultiplexed fastq files were unzipped using the "unzip -q casava-18paired-end-

211   demultiplexed.zip" command, followed by merging individual forward and reverse fastq

212   files into a single fastq file. The Atacama soil microbiome pipeline was incorporated to

213   control demultiplexed paired-end reads using the DADA2 plugin as previously described

214   (Callahan et al., 2016). Low-quality sequences were trimmed and filtered out, and

215   subsequent merging of paired-end reads ensured 20 nucleotide overhangs between

216 forward and reverse reads. Chimeric sequences were removed from the sequence table.

217 The qiime2 feature-classifier plugin v. 7.0 was used for taxonomic assignment against the

218 pre-trained Silva_132_99% classifier (Quast et al., 2013). The "qiime diversity core-

219 metrics-phylogenetic" command was used to compute diversity metrics, after which the

220 "QIIME diversity alpha-group-significance" command was used to explore microbial

221 diversity using Faith_pd and evenness metrics as measures of community richness and

222 evenness, respectively. Raw sequences will be submitted to the required databases.

223 *Functional characterization of microbial communities*

224 To determine the functionality of the microbial genome, we predicted the functional

225 pathways using the Phylogenetic Investigation of Communities by Reconstruction of

226 Unobserved States 2 (PICRUSt2) pipeline. We assigned functional predictions by

227 normalizing the bacterial sequences and OTUs to the KEGG Ortholog (KO) databases

228 and Clusters of Orthologous Groups (COGs) to predict metabolic pathways.

229 *Visualization*

230 Microbiome Analyst, a web-based interface, was used for data visualization using

231 taxonomy and metadata tables generated from data processing as input files (Dhariwal

232 et al., 2017; Chong et al., 2020). Low count and prevalence data were filtered from the

233 OTU table by setting values of 10 and 20, respectively. A filtered abundance table was

234 exported and used in generating histograms of bacterial abundance in Microsoft Excel

235 2016 (Microsoft, 2018). Boxplots of alpha diversity were generated with GraphPad Prism

236 version 8 for Windows (GraphPad Software, La Jolla California USA,

237 www.graphpad.com) using the pairwise table generated from the "qiime diversity alpha-

238 group-significance" command. Network correlation maps were constructed based on the

239 sparse correlations for compositional data (SparCC) approach (Friedman and Alm, 2012).

240 This approach uses the log-transformed values to carry out multiple iterations, which

241 subsequently identifies taxa outliers to the correlation parameters (Chong et al., 2020).

242 To compare the differences in the microbiome between tick groups based on measures

243 of distance or dissimilarity, a matrix was generated from log-transformed sequence data,

244 and ordination of the plots was visualized using both Principal Coordinates Analysis

245 (PCoA) and non-metric multidimensional scaling (NMDS). The Bray–Curtis distance

246 matrix was used to visualize compositional differences in the microbiome across all
247 groups.

248 Statistical Analysis

249 The Wilcoxon rank-sum test estimated significant correlations in diversity indexes across
250 developmental stages and tissue data sets. A Kruskal–Wallis test followed by Dunn's
251 multiple comparison test was used in comparing the effect of blood meal and *R. parkeri*
252 on microbial richness between two different groups (unfed vs. fed or uninfected vs.
253 infected).

254 **Results**

255 *Sequencing results*

256 A total of 91 samples, representing at least three biological replicates across
257 developmental stages (eggs, larvae, nymph, and adult), tissues (salivary gland, midgut,
258 and ovaries), and body fluids (saliva) from uninfected and *R. parkeri*-infected ticks,
259 generated a total of 4,090,811 forward and reverse reads, with a mean of 45,453.5 and
260 a maximum of 112,242 reads per sample (Additional File, Table 1). Rarefaction analysis
261 of the individual samples from a sequencing depth of 500 to 4000 confirmed that there
262 was adequate sequence coverage relative to the number of operational taxonomic units
263 (OTUs) and a plateau for individual tick samples (Additional File, Fig. 1A, B). Overall, 711
264 unique OTUs were identified, with 254 identified from each developmental stage and
265 tissue.

266 *Microbiome dynamics across developmental stages*

267 Proteobacteria represented the most abundant phylum throughout ontogeny, with a
268 relative abundance of 84%, followed by Actinobacteria, Firmicutes, and an
269 uncharacterized phylum (Additional File, Fig. 2A). An extended breakdown of each
270 identified phylum and the number of member bacteria at the genus level is represented
271 using pie charts for each phylum, as shown in Additional File, Fig. 2B–D. The breakdown
272 of the top 10 most frequent bacterial genera shows that *Francisella* and *Rickettsia* were
273 the predominant members of the *Am. maculatum* microbiome across tick developmental

stages (Fig. 1A). We observed a progressive decrease in the relative abundance of the genus *Cutibacterium* throughout each developmental stage, from egg to adult male and female ticks (Fig. 1A). Other bacterial genera, such as *Rhodococcus*, *Pseudomonas*, and *Candidatus_Midichloria*, were also detected at relatively lower abundance. The abundance of representative bacterial genera was also compared between blood-fed and unfed life stages. Uptake of a blood meal was observed to impact the relative abundance of *Francisella* and *Cutibacterium* (Fig. 1B). Following a blood meal, the abundance of *Francisella* was negatively impacted, whereas *Cutibacterium* abundance went up in blood-fed larvae compared with unfed larvae.

Interestingly, opposing trends were observed when blood-fed nymphs were compared with unfed nymphal ticks. The relative abundance of *Cutibacterium* was reduced, whereas *Francisella* abundance was observed to increase (Fig. 1B). To examine the modulation of microbial assemblages in the presence of pathogenic microbes, we compared the relative abundances of bacteria between uninfected and *R. parkeri*-infected samples from each developmental stage. There is a clear trend of decreasing *Francisella* abundance, and a corresponding increase in *Rickettsia* and *Candidatus_Midichloria* across all *R. parkeri*-infected stages compared with uninfected samples (Fig. 1C). Notably, the *Cutibacterium* load was negatively impacted by the presence of *R. parkeri* when infected and uninfected larvae and nymphs were compared (Fig. 1C).

Eggs exhibited higher bacterial richness and evenness, regardless of blood meal or infection (Wilcoxon rank-sum test *p < 0.05*). At the same time, nymphs showed the least microbial richness and evenness (Wilcoxon rank-sum test *p < 0.001*) (Fig. 1D, E). No significant microbial richness in the blood-fed samples was observed; however, blood meal was seen to exert a significant impact on species proportions in unfed nymphs when compared with unfed larvae (Kruskal–Wallis test followed by Dunn's multiple comparison test, *p < 0.05*) and in the fed nymphs compared with unfed larvae (Kruskal–Wallis test followed by Dunn's multiple comparison test, *p < 0.001*) when the Pielou_e evenness index was estimated (Fig. 1F, G) Overall, blood-feeding had no significant effect on microbial richness compared with unfed ticks across developmental stages.

303   The presence of *R. parkeri* infection was not found to affect microbial richness and

304   evenness between developmental stages. However, a reduction in microbial richness in

305   *R. parkeri*-infected nymphs compared with uninfected eggs (Kruskal–Wallis test followed

306   by Dunn's multiple comparison test, *p < 0.05*) and infected eggs (Kruskal–Wallis test

307   followed by Dunn's multiple comparison test, *p < 0.05*) was noted (Fig. 1H). *R. parkeri*

308   infection was seen to reduce species proportion when an uninfected nymphal sample was

309   compared with uninfected egg samples (Kruskal–Wallis test followed by Dunn's multiple

310   comparison test, *p < 0.001*); likewise, when the infected nymphal sample was compared

311   with an uninfected egg sample (Kruskal–Wallis test followed by Dunn's multiple

312   comparison test, *p < 0.05*) and when an uninfected nymphal sample was compared with

313   an infected egg sample (Kruskal–Wallis test followed by Dunn's multiple comparison test,

314   *p < 0.05*) (Figure 1I). NMDS analysis of community structure using the Bray–Curtis (BC)

315   distance matrix (PERMANOVA, F-value = 22.818; R^2 = 0.75015; p-value < 0.001 [NMDS]

316   Stress = 0.12544) revealed two distinct clustering patterns in which the earlier

317   developmental stages (egg, larvae, and a few nymphs) uniquely clustered away from the

318   later developmental stages (male, female, and a few nymphs) (Additional File, Fig. 3).

319   The BC distance matrix measures dissimilarity in microbial communities based on

320   compositional differences among our samples. The observed clustering pattern further

321   supports the differences observed in the presence of *Cutibacterium* in the eggs, larvae,

322   and nymphs but not in adult male and female ticks. Overall, both *Francisella* and

323   *Rickettsia* predominated in the microbiome during the developmental stages. Both blood

324   meal and *R. parkeri* infection negatively affected the abundance of *Francisella,* while

325   blood meal reduced microbial richness in earlier developmental stages.

326   *Microbiome composition and diversity across tissue niches*

327   As with developmental stages, the phylum Proteobacteria had the greatest abundance of

328   bacteria, with a relative abundance of 86%, followed by Firmicutes, Actinobacteria, and

329   an unknown phylum, as illustrated in the Additional File, Fig. 3A–D. Representative

330   sequences generated from tissue samples showed a similar trend to what was found for

331   developmental stages. *Francisella* and *Rickettsia* predominated in the microbiomes of

332   isolated tissues. In addition, the genus *Candidatus_Midichloria* was detected at relatively

333 high abundance across isolated tissues, except for the saliva microbiome, which
334 contained the genus *Bacillus*. By contrast, the genus *Cutibacterium* was present in all
335 tissues, except for ovarian samples (Fig. 2A). Following blood uptake, the proportion of
336 bacteria identified in the partially fed salivary gland was higher than in the unfed salivary
337 gland (Fig. 2B). Interestingly, blood meal reduced the abundance of *Francisella*, whereas
338 the prevalence of *Rickettsia, Cutibacterium,* and *Candidatus_Midichloria* increased (Fig.
339 2B). The effect of blood meal on the microbial abundance in the midgut tissues was
340 different from salivary gland; in the reverse of what was observed in the salivary gland,
341 blood meal increased the relative abundance of *Francisella* and *Candidatus_Midichloria*,
342 while reducing that of *Rickettsia.* Due to the unique developmental trajectory of the female
343 tick, in which ovarian development did not commence until 4–5 days post-blood-feeding,
344 ovarian tissues from unfed female ticks were not included in this analysis (Fig. 2B).
345 Bacterial communities were significantly different between unfed and partially blood-fed
346 salivary gland (PERMANOVA F-value = 22.766; R^2 = 0.7779; p-value < 0.001) and midgut
347 tissues (PERMANOVA F-value = 16.167; R^2 = 0.69785; p-value < 0.001), according to
348 PCoA analysis of the Bray–Curtis distance matrix (Additional File, Fig. 4A, B).

349 The presence of *R. parkeri* was associated with a corresponding increase in the relative
350 abundance of *Candidatus_Midichloria* in all infected compared with uninfected tissues,
351 with a corresponding decrease in the prevalence of *Francisella* (Fig. 2C). There was an
352 increase in the relative abundance of *Rickettsia* detected in *R. parkeri*-infected saliva
353 compared with saliva from uninfected ticks. Bacterial communities were significantly
354 different between uninfected and infected salivary gland (PERMANOVA F-value =
355 20.316; R^2 = 0.75761; p-value < 0.001), midgut (PERMANOVA] F-value = 36.225; R^2 =
356 0.83806; p-value < 0.001) and ovarian tissues (PERMANOVA F-value = 29.509; R^2 =
357 0.89397; p-value < 0.008), according to PCoA analysis of the Bray–Curtis distance matrix
358 (Additional File, Fig. 5A–C).

359 Overall, microbial richness was highest in midgut tissues (Wilcoxon rank-sum test *p <*
360 *0.001*) and lowest in the ovary (Wilcoxon rank-sum test *p < 0.05*), based on the
361 Faith_phylogenetic distance index. At the same time, no significant differences were
362 found in microbial proportions across different tissues, including saliva (Fig. 2D, E). The

363   impact of blood meal on alpha diversity between unfed and partially fed tissues was

364   assessed, and blood meal was found to reduce the species richness following blood

365   uptake in the midgut compared with the unfed midgut (Fig. 2F), while species proportions

366   were not significantly impacted (Fig. 2G). Similarly, there was no significant difference in

367   either species richness or evenness between *R. parkeri*-infected and uninfected tissues

368   (Fig. 2H, I). Here we found that blood meal and *R. parkeri* infection shaped the *Am.*

369   *maculatum* microbiome in a tissue-dependent manner.

370

371   *Microbiota interactions across developmental stages*

372   We performed network analysis to visualize significant positive and negative correlations

373   between the bacterial genera identified. We observed a total of 286 significant partial

374   correlations between 43 bacterial genera, 52% (150) of which showed positive

375   correlations, while the remaining 48% (136) exhibited negative correlations (Additional

376   File, Table 2). All identified bacteria were from the phyla Actinobacteria (10 genera),

377   Firmicutes (12 genera), Spirochaetota (1 genus), Proteobacteria (12 genera),

378   Cyanobacteria (1 genus), Bacteroidota (4 genera), and Fusobacteria (1 genus) as well as

379   an unknown phylum (1 genus) (Fig. 3). The genera *Francisella, Rickettsia,* and

380   *Candidatus_Midichloria* were found within the same network cluster where they share

381   significant positive correlations. Individually, they both interacted with other bacteria

382   genera as is the case with *Francisella* and *Rickettsia* OTUs sharing negative correlations

383   with *Listeria, Coxiella, Bacillus, and Enterococcus,* and positive correlations with

384   Cutibacterium. The genus *Candidatus_Midichloria* on the other hand was positively

385   correlated with OTUs belonging to the *Mitochondria* genus. It is worth noting that

386   *Candidatus_Midichloria* had fewer taxa with which it interacted than *Francisella or*

387   *Rickettsia* (Additional File, Table 2). Another interesting observation made from the

388   network interactions was the significant negative correlations in the interactions between

389   *Coxiella* and *Francisella* and between *Coxiella* and *Rickettsia*. A more surprising

390   correlation was identified between *Bacillus, Listeria, Enterococcus,* and *Staphylococcus*,

391   all of which are members of the phylum Firmicutes. They were all negatively correlated

392   with *Rickettsia*, *Francisella,* and *Candidatus_Midichloria* from Proteobacteria (Fig. 3). To

393   identify the significantly represented microbial genera between different life stages, we

394   used linear discriminant analysis effect size (LEfSe) to determine the respective LDA

395   scores for the identified bacteria observed in the samples. LDA analysis showed that, out

396   of 46 bacteria taxa, 13 were significantly correlated at different life stages. Several of the

397   bacteria either increased or decreased in more than one life stage. By contrast, the

398   bacterial taxon *Enhydrobacter* is the only genus represented exclusively at the egg stage

399   (Additional File, Table 3). Likewise, the taxa *Enterococcus, Lactobacillus,* and *Coxiella*

400   were not detected at any developmental stages. Another interesting observation was the

401   increased presence of the genera *Corynebacterium* and *Cutibacterium* exclusively at

402   early developmental stages (Additional File, Fig. 4).

403   *Tissue-driven microbial interactions*

404   Network analysis in tissues showed 220 significant correlations between 46 bacterial

405   genera, each belonging to the phyla Proteobacteria (20 genera), Firmicutes (13),

406   Actinobacteriota (6 genera), Cyanobacteria (2 genera), Bacteroidota (3 genera), and

407   Fusobacteriota (1 genus) as well as an unknown phylum (1 genus). Seventy-two (33%)

408   were negative correlations, while 148 (67%) were positive correlations (Additional File,

409   Table 4). We observed that OTUs belonging to *Candidatus_Midichloria, Francisella* and

410   *Rickettsia* were positively correlated and represent a network cluster that shares both

411   positive and negative correlations with OTUs from other bacteria genera. Interestingly,

412   bacteria belonging to the phylum Firmicutes, such as *Listeria, Staphylococcus, Bacillus,*

413   *and Enterococcus* were negatively correlated with *Francisella, Rickettsia,* and

414   *Candidatus_Midichloria* which are bacteria from the Proteobacteria phylum (Fig. 4). LDA

415   analysis revealed that *Francisella* was significantly enriched in ovaries and salivary

416   glands, whereas *Rickettsia* was increased significantly in the midgut tissues and saliva

417   (Additional File, Table 5; Fig. 5). The saliva microbiome was also the only sample

418   exclusively enriched with *Alcaligenes, Moraxella, Pseudomonas,* and *Spiroplasma*. The

419   first three belong to the phylum Proteobacteria and the latter from the phylum Firmicutes.

420   *Microbial interactions in the salivary gland*

421   A total of 608 significant partial interactions between 48 bacteria genera were identified

422   in network analysis of the salivary gland, with 176 (29%) negative correlations and 432

423   (71%) positive correlations (Additional File, Table 6). Most interactions were seen with

424   *Francisella, Rickettsia,* and *Candidatus_Midichloria* (Fig. 5). The most surprising

425   correlation   was   the   negative   correlation   observed   between   *Rickettsia*   and

426   *Candidatus_Midichloria*, and the most interesting was that *Rickettsia* shares a correlation

427   network only with *Candidatus_Midichloria* (Fig. 5). No direct interaction was observed

428   between *Francisella* and *Candidatus_Midichloria* or between *Francisella* and *Rickettsia*.

429   LDA analysis of significantly enriched bacteria revealed a unique pattern between *R.*

430   *parkeri*-infected and uninfected salivary glands. Uninfected salivary glands were

431   exclusively   enriched   with   *Francisella, Bacillus, Cutibacterium, Pseudomonas,*   and

432   *Stenotrophomonas.*   By   contrast,   the   genera   *Enterococcus,   Rickettsia,*   and

433   *Candidatus_Midichloria* were the only bacteria significantly enriched in *R. parkeri*-infected

434   salivary glands (Additional File, Fig. 6A). Interestingly, *Francisella* was the only bacterium

435   identified as significantly enriched in the unfed salivary gland. While *Francisella* was also

436   enriched in the partially fed salivary gland, several other bacteria were identified, such as

437   *Escherichia_Shigella, Bacillus, Staphylococcus, Enterococcus, Cutibacterium,* and

438   *Pseudomonas* (Additional File, Fig. 6B).

Microbial interaction in the midgut

440   We observed many fewer (56) significant partial correlations in the midgut tissues

441   between 29 bacteria genera, all belonging to the phyla Proteobacteria (15 genera),

442   Firmicutes (3 genera), Actinobacteriota (4 genera), Cyanobacteria (1 genus), and

443   Bacteroidota (2 genera) as well as an unknown phylum (1 genus), 16 (29%) of which

444   were negative correlations and the remaining 40 (71%) positive correlations (Additional

445   File, Table 7). The network map of bacterial interactions identified five distinct networks,

446   with *Rickettsia* and *Candidatus_Midichloria* observed to be part of the same network with

447   positive correlations. *Francisella* was found to be in a different network (Fig. 6). A striking

448   observation was the ubiquitous presence of bacteria in the phylum Proteobacteria across

449   all five identified networks (Fig. 6). The LDA score from LEfSe identified the enrichment

450   of *Rickettsia, Escherichia_Shigella,* and *Cutibacterium* in both uninfected and *R. parkeri*-

451   infected midgut tissues. Compared with the *R. parkeri*-infected midgut, only *Francisella*

452   was significantly enriched in the uninfected midgut, while *Bacillus* was enriched in the *R.*

453 *parkeri*-infected midgut (Additional File, Fig. 6A). Assessing the effect of blood meal on

454 bacterial enrichment identified a shared enrichment of *Rickettsia, Escherichia_Shigella,*

455 and *Cutibacterium* in both unfed and partially fed midgut. We observed *Pseudomonas*

456 and *Brevibacterium* in the unfed midgut, while *Francisella* and *Staphylococcus* were

457 enriched in partially blood-fed midgut tissues (Additional File, Fig. 6B). Microbiota–

458 microbiota interactions across developmental stages were driven mainly by three of the

459 most abundant bacteria: *Francisella, Rickettsia,* and *Candidatus_Midichloria*. Other

460 interactions revealed that certain taxonomic groups were inversely correlated, as seen

461 between the phyla Firmicutes and Proteobacteria. Many specific interactions were

462 observed in the tissues, suggesting tissue-dependent influences on how microbes

463 interact in different tissue niches.

464 *Functional characterization of bacterial communities*

465 Functional prediction of microbiota genes compared with COG functional categories

466 identified genes involved in ribosomal structure and biogenesis, nucleotide transport, and

467 metabolism as the most abundant across developmental stages (Additional file, Table 8).

468 Several genes involved in metabolisms, such as lipid transport, coenzyme transport,

469 amino acid transport, and carbohydrate transport, were also identified (Additional files,

470 Fig. 10). Prediction of metabolic genes and pathways using the KEGG Orthology (KO)

471 categories assigned 19% of the metabolic functions to genes in carbohydrate metabolism

472 pathways and 18% of the functions were encoded by genes in amino acid metabolism

473 pathways. By comparison, genes encoding cofactors in the vitamin metabolism pathways

474 and energy metabolism pathways represented 15% and 13% of the metabolic pathways,

475 respectively (Additional file, Fig. 10).

476 Differences in functional community profiles within the metabolic pathways were further

477 examined between the different feeding stages and infection status across dissected

478 tissues based on the KEEG metabolism categories. The partially fed salivary gland and

479 midgut had a higher proportion of sequences assigned to energy metabolism and

480 carbohydrate metabolism than the unfed salivary gland and midgut (Fig. 7A, B). The

481 presence of *R. parkeri* led to an increase in the proportion of glycan biosynthesis and

482 metabolism genes, carbohydrate metabolism genes, and genes involved in the

483   metabolism of cofactors and vitamins in the salivary glands. A slight increase was also

484   seen in genes involved in the metabolism and biodegradation of xenobiotics in the *R.*

485   *parkeri*-infected salivary gland (Fig. 8A). A slight increase in the proportion of energy

486   metabolism genes was associated with *R. parkeri* in infected midgut compared with the

487   uninfected midgut (Fig. 8B). Interestingly, genes involved in amino acid metabolism were

488   seen to be reduced in *R. parkeri*-infected salivary glands and midgut compared with

489   uninfected tissues (Fig. 8A, B). No differences between metabolic predictions were

490   detected between *R. parkeri*-infected and uninfected ovarian tissues (Additional file, Fig.

491   11).

492   **Discussion**

493   This study is the first to characterize microbiome changes throughout the ontogeny of the

494   Gulf Coast tick, a competent vector of the spotted fever group rickettsiae, *R. parkeri*.

495   Using a high-throughput metagenomic approach that allowed us to barcode DNA

496   extracted from individual ticks and process them in a single run, the present study set out

497   with the aim of assessing the core microbial assemblages present in *Am. maculatum* ticks

498   and determine the changes under certain physiological conditions vis-à-vis development,

499   hematophagy, and pathogen infection. The results show that changes to the core

500   microbiome occur in response to a blood meal and pathogen association but not as a

501   function of the developmental stage. Similarly, as expected, microbe-microbe interactions

502   depended on the specific tick tissues in which those interactions took place.

503   **The *Amblyomma maculatum* microbiome remains stable across ontogeny**

504   The typical life cycle of *Am. maculatum* ticks encompass critical physiological and

505   environmental events conferred by intrinsic and extrinsic factors, such that the

506   persistence of the microbiome and every similar micro-community that utilizes the tick as

507   a microenvironment across these dynamic events is continuously tested. Two very well-

508   studied factors that exert significant pressure on the tick microbiome are blood meal and

509   pathogen replication (Abraham et al., 2017; Swei and Kwan. 2017; Adegoke et al., 2020;

510   Wei et al., 2021), albeit with varying outcomes reported. In the current study, a shift

511   favoring the establishment of a single bacterial genus along developmental lines (eggs to

512   adult male and female) is exhibited (Fig. 1A–C). Even so, the uptake and breakdown of

513 nutritious blood meals and the intricacies of tick–pathogen interactions involve several
514 detailed mechanistic processes that have been shown to significantly impact tick
515 physiology (de la Fuente et al., 2016; Hoxmeier et al., 2017; Budachetri et al., 2018), the
516 current study shows that members of the *Am. maculatum* microbial communities exhibit
517 reduced plasticity thus maintaining a stable microbial core. This observation raises the
518 question of whether the tick microbiome is self-regulated in ticks and tick tissues

519 Notably, while the core microbiome persists across developmental stages, certain
520 bacterial genera were found to be associated with both blood meal and pathogen
521 infection, as seen with *Cutibacterium* and *Candidatus_Midichloria*, and whether the
522 introduction of these bacteria in fewer numbers significantly impacts overall tick biology
523 is a question beyond the scope of this study (Budachetri et al., 2018; Adegoke et al.,
524 2020, Abraham et al., 2017). To further understand how changes across tick
525 developmental stages shape microbial assemblages, it is imperative to assess microbial
526 assemblages and community measures of diversity, such as richness and evenness
527 (Brown et al., 2020). Community diversity is important because the smallest differences
528 at the taxon level induced by blood meal or pathogen interaction could interfere with
529 community structure, which would otherwise not be reflected in the abundance profile.
530 We observed a continuous decrease in community diversity towards later developmental
531 stages (Figure 1D–I). For both diversity metrics employed, a reduction in community
532 richness likely indicated a corresponding decline in all or certain specific bacterial taxa.
533 At the same time, a decrease in evenness would imply that certain bacterial taxa are
534 allowed to increase in abundance at the expense of other bacteria. This finding is
535 consistent with observations made in the kissing bugs, where there is a decrease in
536 diversity associated with ontogenic development (Mann et al., 2020), which is in
537 disagreement with Oliveira et al. (2018), who reported an increase in diversity with
538 ontogenic development. A possible explanation for this discrepancy may be attributed to
539 internal and external changes that occur during metamorphosis. Shedding of the midgut
540 lining and the external cuticles are two of the most important phenomena during
541 development. These may come with significant loss of resident and non-obligate bacteria
542 whose absence poses no detrimental effect on tick biology (Philipp et al., 2013). There
543 are, however, other possible explanations for the reduction in diversity seen in this study.

544 One such explanation is that bacteria that are not vertically maintained from the female
545 to her eggs are replaced by vertically maintained bacteria. The preservation of vertically
546 maintained species would explain the loss of *Cutibacterium* in adult male and female
547 ticks. By extension, there would be a reduction in overall diversity. Previous findings have
548 highlighted the importance of initial exposure to bacteria in eliciting a robust immune
549 response upon subsequent exposure to the same bacteria or bacteria from a similar
550 group, a phenomenon referred to as immune priming (Trappeniers et al., 2019; Powers
551 et al., 2020). This could explain the fact that immature developmental stages of ticks are
552 easily infected with bacteria from the environment because of their naïve immune status.
553 These bacteria will not be carried over to the adult stage due to a more developed immune
554 status. The persistence of *Francisella, Rickettsia,* and *Candidatus_Midichloria* to the adult
555 male and female further emphasizes their position as candidates for vertical maintenance,
556 as previously reported for bacterial species from the same genus (Baldridge et al., 2009;
557 Wright et al., 2015; Azagi et al., 2017; Mukhacheva and Kovalev, 2017; Budachetri et al.,
558 2018).

559 ***Microbial assemblages in tissues are driven by pathogen and host blood***

560 To gain in-depth insight into how different arthropod tissues contribute to tick biology and,
561 most importantly, their role in vector competence, it is imperative to know how resident
562 microbial communities differ from one tissue to the other. Several factors have been
563 identified that significantly affect how the microbiome is shaped in different arthropod
564 tissues, albeit with varying outcomes and findings. In this study, we asked whether
565 differences in microbial composition occur within tissues and whether changes influence
566 these differences in the state of blood-feeding and infection status. Our results clearly
567 show a difference in the abundance and composition of the bacteria identified across tick
568 tissues. A fascinating conclusion from our findings is the higher bacterial proportion in
569 saliva, which does not correspond to the bacterial balance in the salivary glands. Tick
570 saliva contains simply a snapshot of the microbes secreted by the tick and is possibly not
571 a good representation of all microbes delivered during prolonged feeding. These
572 differences can be explained in part by the fact that some of the microbial populations
573 identified in the saliva, such as *Bacillus* and *Staphylococcus,* are known environmental

574 bacteria, have also been reported to be found on the skin and fur of the animal hosts
575 (Dastgheyb and Otto, 2015; Onyango and Alreshidi, 2018; Ravine, 2019), and may have
576 been acquired during the feeding process. Some of these bacteria could also have been
577 mechanically transferred during saliva collection from the ticks. The presence of the
578 microbiome within tick saliva, while preliminary, could implicate the tick microbiome in
579 modulating the host immune response to tick bite at the host–tick interface. The
580 observation of a higher diversity seen in midgut tissues compared with salivary gland,
581 ovary, and saliva contrasted with the findings of Zolnik et al. (2016), who reported a higher
582 diversity in salivary gland compared with midgut tissue. The tick midgut and associated
583 peritrophic membrane play an important role in blood breakdown and its components by
584 several catalytic proteins. The production of toxic reactive oxygen species (ROS) and
585 reactive nitrogen species (RNS), which follow blood digestion, is also dampened by these
586 midgut proteins, thus enabling midgut-resident microbial replication. The heme
587 component of the blood meal derived by catalytic proteins also counters the potential
588 tissue damage associated with a heme-induced oxidative burst. Another plausible
589 explanation for the higher microbial diversity observed in the midgut reported from this
590 study is that the midgut is the only tissue that directly encounters host blood, and it
591 provides the first line of contact with any bacterium coming in with the blood meal (Houk,
592 1977; Tarnowski and Coons, 1989; Gaio et al., 2011; Lejal et al., 2019). However,
593 prolonged blood feeding and, by extension, the initiation of blood meal digestion might
594 provide an enabling environment for bacterial replication and growth, hence impacting the
595 dynamic and increasing overall diversity of the midgut microbiome as seen from this
596 study. Due to the importance of the ovarian tissues in developmental success, it is
597 expected that several physiological barriers will be put in place to confer protection and
598 reduce the tick's interaction with circulating microbes to the barest minimum. The reduced
599 microbial diversification observed in the ovary is consistent with this, as seen in Fig. 2D.
600 Several studies have outlined the contribution of invertebrate hemocytes to immune
601 functions while also identifying distinct populations of hemocytes as either circulating or
602 sessile (Kadota et al., 2003; King et al., 2013; Sigle and Hillyer, 2018). The sessile
603 population of hemocytes is usually found attached to cavity walls, such as the abdomen,
604 thorax, and internal organs. While extensive studies have described how arthropod

605   hemocytes play a significant role in immunomodulation (Pereira et al., 2001; Hillyer, 2009;

606   Liu et al., 2011; Hillyer and Strand, 2014; Fiorotti et al., 2019; Kwon et al., 2019), few

607   studies have defined the functional role of sessile populations in the biology of the

608   organism (Sigle and Hillyer, 2016). Hence, it could be hypothesized that circulating or

609   sessile hemocytes would form immunological barriers as part of an extensive

610   physiological barrier to protect a vital organ, such as the ovary, as seen with several

611   human and mammalian blood–tissue barriers (Fröhlich, 2002)

612   It has already been established that blood uptake, which usually lasts several days in

613   ticks, can introduce a plethora of pathogenic and non-pathogenic microbes into ticks

614   (Bhatia et al., 2018; Zolnik et al., 2018; Landesman et al., 2019). While ticks acquire host

615   blood for nutritional requirements, several host factors present in the blood meal could

616   also potentially contribute to compositional changes that are likely to occur to the

617   microbiome throughout the extended feeding process. For instance, the tick midgut

618   responds to the presence of the blood meal via intricate protein expression patterns

619   (Rachinsky et al., 2008; Schwarz et al., 2014; Perner et al., 2016; Oleaga et al., 2017; Liu

620   et al., 2018) while also undergoing certain morphological and structural adjustments

621   (Tarnowski and Coons, 1989; Frants et al., 2010), all of which could have an impact on

622   the microbial environment in the midgut, as previously reported (Zhang et al., 2014; Zolnik

623   et al., 2018; Landesman et al., 2019). Results from our study show that microbial diversity

624   is impacted following uptake of the blood meal in both salivary gland and midgut tissues

625   (Fig. 2E). We also observed a combinatorial effect of blood meal and *R. parkeri* infection

626   in reducing the abundance of *Francisella* while increasing *Rickettsia* abundance in the

627   partially fed and infected salivary gland and, vice-versa, in the partially fed and infected

628   midgut. This suggests that there is the trafficking of *Rickettsia* from the midgut into the

629   salivary gland during feeding. While studies that assessed the impact of blood meal on

630   the tick microbiome are limited to developmental stages, it is interesting to note that our

631   studies corroborate a great number of these studies, albeit in life stages. Zolnik and

632   colleagues (2016) observed a significant reduction in alpha-diversity throughout the

633   feeding period of nymphal ticks compared with the unfed nymphs of black-legged ticks,

634   and Zhang et al. (2014) also reported an altered microbial composition following a

635   prolonged blood meal in *Ixodes persulcatus* ticks. A similar observation was reported in

636 the malaria mosquito, in which Muturi et al. (2019) found a significant decrease in
637 microbial diversity in blood-fed *Aedes aegypti* compared with sugar-fed *Ae. aegypti*
638 mosquitoes. While comparing the effect of different host blood meal sources was beyond
639 the scope of this study, our findings strongly implicate host blood meal as a significant
640 factor in driving tick microbiome diversity, which may pose a significant effect on tick
641 biology, as previously shown by Swei and Kwan, 2016.

642 ***Microbe–microbe interactions are driven by the specific host tissue and not the***
643 ***developmental stage***

644 *Microbial interactions across developmental stages*

645 The biological success of the tick as a hematophagous arthropod and a vector of disease
646 pathogens hinges partly on the specific interactions between different members of the
647 resident microbiota, which encompasses the entirety of all the microorganisms present in
648 an environment. Identifying unique interactions between these microbial community
649 members is a critical step in developing effective control measures against tick-
650 transmitted pathogens.

651 Our network analysis on the overall dataset across all developmental stages identified
652 similar percentages of positive and negative correlations, suggesting a much more
653 balanced distribution of both antagonistic (Budachetri et al., 2018) and synergistic (Eiler
654 et al., 2012; Chow et al., 2014) interactions between members of the microbial
655 communities. This observation contrasts with a recent study by Lejal et al. (2021), who
656 reported more than 97% partial positive correlations across all the datasets in *Ixodes*
657 *ricinus* ticks and suggested that most of the tick microbial community favors a mutualistic
658 interaction. While the findings of our study contrast with this observation, it should be
659 stated that microbial correlations of an individual organism may not fully represent
660 interactions in different tissue niches, which are often a microenvironment for unique
661 bacteria communities (Pollet et al., 2020). The genera *Rickettsia*, *Francisella,* and
662 *Candidatus_Midichloria* were all part of the same network, with positive correlations
663 between all three bacterial genera, and these were previously identified in *Am. maculatum*
664 ticks (Budachetri et al., 2014; Budachetri et al., 2018) and *Ix. ricinus* ticks (Lejal et al.,

665 2021). At the same time, *Francisella* and *Candidatus_Midichloria* are major
666 endosymbionts found in the *Am. maculatum* microbiome and Budachetri et al., (2018)
667 reported an increase in *Candidatus_Midichloria* load following *R. parkeri* infection,
668 proposing a positive correlation between these bacteria and a corresponding reduction in
669 *Francisella* load following *R. parkeri* infection, implying a negative correlation.

670 Interestingly, recent network analysis on the *Ix. ricinus* microbiota also shows a positive
671 correlation between *Rickettsia* and *Candidatus_Midichloria* OTUs, indicating a facilitative
672 interaction between these bacteria (Lejal et al., 2021). Our data suggest a positive
673 interaction between the pathogenic Rickettsia and the obligate endosymbiont
674 *Candidatus_Midichloria*. The current study's findings are consistent with those of
675 Budachetri et al. (2018), who reported a synergistic interaction between *R. parkeri* and
676 *Candidatus_Midichloria mitochondrii* and an antagonistic interaction between *R. parkeri*
677 and a *Francisella*-like endosymbiont. While identification at the species level exceeded
678 the resolution of our sequencing analysis, we have strong reason to believe that the OTU
679 belonging to the *Coxiella* genus is the *Coxiella*-like endosymbiont (CLE), because the
680 ticks used in this study were strictly maintained under laboratory conditions. CLE is
681 ubiquitously present in most hard ticks, with reports suggesting an obligate association
682 with the tick host, in which they provide essential vitamin supplements for tick
683 physiological success (Duron et al., 2015; Smith et al., 2015; Guizzo et al., 2017; Ben-
684 Yosef et al., 2020).

685 A recent study reported the replacement of bacteria in the *Coxiellaceae* family with those
686 in the *Francisellaceae* family in both lab-maintained and field-collected *Am. americanum*
687 ticks (Kumar et al., 2021), providing further evidence of competition between these two
688 tick endosymbionts. The strict adherence to a single nutritional mutualist by tick species
689 is an area of tick–microbial interaction that requires further exploration, and future studies
690 should aim at characterizing both the immunoproteome and metabolites of gnotobiotic
691 ticks with known obligate endosymbionts. Other key interactions observed between the
692 OTUs belong to the *Bacillus*, *Rickettsia,* and *Francisella* genera. The genus *Bacillus* is an
693 environmental resident microbe that ticks acquire while questing in the environment and
694 during the attachment process to the host (Ross et al., 2019). We observed negative

695 correlations between *Bacillus* and *Rickettsia* and between *Bacillus* and *Francisella,*
696 suggesting a competitive interaction between these bacterial OTUs. The findings of the
697 current study are consistent with those of another study (Lejal et al., 2021) that described
698 a positive correlation between *Bacillus* and *Rickettsia* but was not compatible with the
699 presence of a high abundance of *Bacillus* in *Theileria*-positive *Rhipicephalus microplus*
700 ticks, as previously described (Adegoke et al., 2020). The factors that favor the
701 establishment and long-term association of environmentally acquired bacteria by ticks still
702 need to be experimentally identified. Whether these bacteria express effector molecules
703 that suppress pathogenic microbes, such bacteria may be utilized as effective vector-
704 control tools in the future to develop paratransgenic ticks.

705 *Microbial interactions are driven by the specific tissue niche*

706 Network analysis on datasets representing all tissues was initially carried out, thereby
707 identifying 67% positive correlations between different bacteria in the networks. We
708 identified more positive correlations across tissue levels than developmental stages,
709 suggesting a much finer association scale at smaller niches (Pollet et al., 2020). Aside
710 from the higher proportion of positive correlations, most of the microbial networks
711 identified when applied to the combined tissue dataset were like those presented for
712 developmental stages. For instance, OTUs from *Francisella, Rickettsia, and*
713 *Candidatus_Midichloria* were all present in the combined tissue networks, including the
714 salivary gland and midgut. Interestingly, while the salivary gland dataset had a relatively
715 higher proportion of networks, it contained more positive correlations (71%). Only OTUs
716 belonging to the genera *Francisella, Rickettsia,* and *Candidatus_Midichloria* were
717 involved in most interactions. An unexpected outcome from the salivary gland network
718 was the observation of a negative correlation between *Rickettsia* and
719 *Candidatus_Midichloria* OTUs, while there was no direct correlation between *Francisella*
720 and either of *Rickettsia* or *Candidatus_Midichloria*. We proposed that
721 *Candidatus_Midichloria* in the salivary gland was not transmitted to the host, due to its
722 restricted location in the mitochondria, hence its absence from the saliva. This
723 phenomenon was also observed in the midgut, albeit with fewer and more distinctly
724 separated microbial networks. A handful of studies deciphered specific correlations

725   between microbial members residing in arthropod vectors (Lejal et al., 2021; Hedge et
726   al., 2018). While our findings here are preliminary at best, they emphasize that tissue-
727   specific microbial interactions do exist, and this should be further investigated, as they
728   may lead to new insights into pathogen replication and establishment across tick tissues.
729   Future work should be targeted towards experimental validation of the predicted
730   correlations to understand how these interactions are shaped.

731   The metabolic predictions based on the microbiota showed no differences in metabolic
732   genes across developmental stages; however, we identified a diverse category of genes
733   involved in metabolic pathways, most of which have been previously reported in ticks and
734   other blood-feeding arthropods (Obregon et al., 2019; Bahrndorff et al., 2018; Jing et al.,
735   2020; Couper et al., 2019). The presence of energy metabolism genes and pathways in
736   higher abundance in the partially fed than the unfed salivary gland and midgut tissues did
737   not completely align with the microbial changes induced by blood meal, especially with
738   the midgut. We saw a significant increase in the microbial profiles in the partially fed
739   salivary gland compared with the unfed salivary gland (Fig. 2B). We hypothesize that
740   since the increased proportion of bacterial genes was involved in energy metabolism,
741   carbohydrate metabolism could be a physiological pressure on the salivary gland as a
742   secretory organ involved in blood meal at the host–feeding interface. The slight increase
743   in the number of genes involved in xenobiotic degradation and metabolism in the partially
744   fed salivary gland could be due to the constant need to counter host immune responses
745   to achieve hematophagy.

746   Interestingly, metabolic pathways involved in energy metabolism and the metabolism of
747   vitamins and cofactors were upregulated in *R. parkeri*-infected salivary glands and midgut
748   tissues (Fig. 8A, B). These changes were also similar to those associated with uptake of
749   blood meal. While we could not tease out whether these changes were solely associated
750   with either blood meal or *R. parkeri* infection, we saw a slight increase in the abundance
751   of genes involved in nucleotide metabolism pathways in the *R. parkeri*-infected salivary
752   gland. The importance of nucleotide metabolism pathways in bacteria is highlighted by
753   their role in bacterial physiological processes and the synthesis of new nucleic acids
754   necessary for replication (DNA) and transcription (RNA) (Lopatkin and Yang, 2021). Our

755 current results show that blood meal increases the relative abundances of *Francisella*
756 and *Candidatus_Midichloria* endosymbionts. Likewise, the abundance of *Rickettsia* also
757 increases with *R. parkeri* infection, suggesting an overall increase in the replication of
758 these bacterial groups, thus leading to an overall increase in nucleic acid replication and
759 transcription. While our functional analysis is predictive at best, with approximately 85%
760 similarity with shotgun metagenomics, it did provide comprehensive insight into the
761 different functional pathways present in the tick microbiota.

762 **Conclusion**

763 The microbiome of *Am. maculatum* comprises ten bacterial genera. Three genera,
764 including *Rickettsia, Francisella*, and *Candidatus_Midichloria,* predominate in the core
765 microbiome. Blood-feeding behavior aided in the proliferation of these three bacteria,
766 whereas overall diversity and evenness were reduced due to elevated levels of ROS
767 associated with blood meal acquisition and digestion, both in whole ticks and in particular
768 organs (gut/salivary glands/ovaries). *R. parkeri* infection co-proliferates with
769 *Candidatus_Midichloria,* while an antagonistic interaction with the *Francisella* genus was
770 observed in the tick life cycle. *R. parkeri* infection further increased the diversity or
771 evenness of the core microbiome. A significant increase in activity of the genes related to
772 metabolic pathways was observed in ticks after a blood meal and pathogen infection. With
773 these results in mind, further study should focus on the interplay between these three
774 bacterial species, including the pathogen, while studying tick–pathogen interactions. The
775 interplay of symbiotic bacteria (*Candidatus_Midichloria/Francisella*) with pathogenic *R.*
776 *parkeri* should yield important findings in future studies.

777

783 **Declarations**

784

Funding

Author Information

**School of Biological, Environmental, and Earth Sciences, University of Southern
Mississippi, Hattiesburg, MS 39406, USA**

Abdulsalam Adegoke, Deepak Kumar, Khemraj Budachetri, Shahid Karim

**Center for Molecular and Cellular Biosciences, University of Southern
Mississippi, Hattiesburg, MS 39406, USA**

Shahid Karim

812 **Abbreviations**

813 *Am. maculatum*: *Amblyomma maculatum*

814 PCA: Principal component analysis

815 OTU: Operational taxonomic unit

816 TBD: Tick-borne disease

817 TBP: Tick-borne pathogens

818 FLE: *Francisella*-like endosymbiont

819 CMM: *Candidatus Midichloria mitochondrii*

820 QIIME2: Quantitative Insights into microbial ecology 2

821 SparCC: sparse correlations for compositional data

822 LEfSe: linear discriminant analysis effect size

823 LDA: linear discrimination analysis

824

825

826

827

828

829

830

831

832

833

834

835

836 Et**hical Approval and Consent to participate**

837 Not applicable.

838

839 **Consent for publication**

840 Not applicable

841 **Availability of data and materials**

842 Raw sequences for this study were submitted to the NCBI read under SRA database and

843 an accession # obtained.

844
845 **Competing interests**

846
847 The authors declare that they have no competing interests.

848
849 **Author contributions**

850
851 Conceptualization: Shahid Karim
852 Data curation: Abdulsalam Adegoke, Deepak Kumar, Shahid Karim
853 Formal analysis: Abdulsalam Adegoke, Deepak Kumar, Shahid Karim
854 Funding acquisition: Shahid Karim
855 Investigation: Abdulsalam Adegoke, Shahid Karim
856 Methodology: Abdulsalam Adegoke, Deepak Kumar, Khemraj Budachetri
857 Project administration: Shahid Karim
858 Resources: Shahid Karim
859 Supervision; Shahid Karim
860 Validation: Abdulsalam Adegoke, Shahid Karim
861 Visualization: Abdulsalam Adegoke
862 Writing, original draft: Abdulsalam Adegoke, Shahid Karim
863 Writing, review & editing: Abdulsalam Adegoke, Deepak Kumar, Khemraj Budachetri,
864 Shahid Karim

865

866

867

868

869

References

1. Abraham, N. M., Liu, L., Jutras, B. L., Yadav, A. K., Narasimhan, S., Gopalakrishnan, V., Ansari, J. M., Jefferson, K. K., Cava, F., Jacobs-Wagner, C., & Fikrig, E. (2017). Pathogen-mediated manipulation of arthropod microbiota to promote infection. Proceedings of the National Academy of Sciences of the United States of America, 114(5), E781–E790. https://doi.org/10.1073/pnas.1613422114

2. Adegoke, A., Kumar, D., Bobo, C., Rashid, M. I., Durrani, A. Z., Sajid, M. S., & Karim, S. (2020). Tick-Borne Pathogens Shape the Native Microbiome Within Tick Vectors. Microorganisms, 8(9), 1299. https://doi.org/10.3390/microorganisms8091299

3. Azagi, T., Klement, E., Perlman, G., Lustig, Y., Mumcuoglu, K. Y., Apanaskevich, D. A., & Gottlieb, Y. (2017). Francisella-Like Endosymbionts and Rickettsia Species in Local and Imported Hyalomma Ticks. Applied and environmental microbiology, 83(18), e01302-17. https://doi.org/10.1128/AEM.01302-17

4. Bahrndorff, S., de Jonge, N., Hansen, J.K. et al. Diversity and metabolic potential of the microbiota associated with a soil arthropod. Sci Rep 8, 2491 (2018). https://doi.org/10.1038/s41598-018-20967-0

5. Baldridge, G. D., Scoles, G. A., Burkhardt, N. Y., Schloeder, B., Kurtti, T. J., & Munderloh, U. G. (2009). Transovarial transmission of Francisella-like endosymbionts and Anaplasma phagocytophilum variants in Dermacentor albipictus (Acari: Ixodidae). Journal of medical entomology, 46(3), 625–632. https://doi.org/10.1603/033.046.0330

6. Ben-Yosef, M., Rot, A., Mahagna, M., Kapri, E., Behar, A., and Gottlieb, Y. (2020). Coxiella-Like Endosymbiont of *Rhipicephalus sanguineus* Is Required for Physiological Processes During Ontogeny. *Front. Microbiol.* 11. doi:10.3389/fmicb.2020.00493.

7. Bhatia, B., Hillman, C., Carracoi, V., Cheff, B. N., Tilly, K., & Rosa, P. A. (2018). Infection history of the blood-meal host dictates pathogenic potential of the Lyme disease spirochete within the feeding tick vector. PLoS pathogens, 14(4), e1006959. https://doi.org/10.1371/journal.ppat.1006959

8. Bolyen, E., Rideout, J.R., Dillon, M.R. et al. Reproducible, interactive, scalable and extensible microbiome data science using QIIME 2. Nat Biotechnol 37, 852–857 (2019). https://doi.org/10.1038/s41587-019-0209-9

9. Bonnet, S. I., & Pollet, T. (2021). Update on the intricate tango between tick microbiomes and tick-borne pathogens. Parasite immunology, 43(5), e12813. https://doi.org/10.1111/pim.12813

10. Bonnet, S. I., Binetruy, F., Hernández-Jarguín, A. M., & Duron, O. (2017). The Tick Microbiome: Why Non-pathogenic Microorganisms Matter in Tick Biology and Pathogen Transmission. Frontiers in cellular and infection microbiology, 7, 236. https://doi.org/10.3389/fcimb.2017.00236

11. Boulanger, N., & Wikel, S. (2021). Induced Transient Immune Tolerance in Ticks and Vertebrate Host: A Keystone of Tick-Borne Diseases?. Frontiers in immunology, 12, 625993. https://doi.org/10.3389/fimmu.2021.625993

12. Brinkerhoff, R. J., Clark, C., Ocasio, K., Gauthier, D. T., & Hynes, W. L. (2020). Factors affecting the microbiome of Ixodes scapularis and Amblyomma americanum. PloS one, 15(5), e0232398. https://doi.org/10.1371/journal.pone.0232398

13. Brown, J.J., Rodríguez-Ruano, S.M., Poosakkannu, A. et al. Ontogeny, species identity, and environment dominate microbiome dynamics in wild populations of kissing bugs (Triatominae). Microbiome 8, 146 (2020). https://doi.org/10.1186/s40168-020-00921-x

14. Budachetri, K., & Karim, S. (2015). An insight into the functional role of thioredoxin reductase, a selenoprotein, in maintaining normal native microbiota in the Gulf Coast tick (Amblyomma maculatum). Insect molecular biology, 24(5), 570–581. https://doi.org/10.1111/imb.12184

15. Budachetri, K., Browning, R. E., Adamson, S. W., Dowd, S. E., Chao, C. C., Ching, W. M., & Karim, S. (2014). An insight into the microbiome of the Amblyomma maculatum (Acari: Ixodidae). Journal of medical entomology, 51(1), 119–129. https://doi.org/10.1603/me12223

16. Budachetri, K., Kumar, D., & Karim, S. (2017). Catalase is a determinant of the colonization and transovarial transmission of Rickettsia parkeri in the Gulf Coast

tick Amblyomma maculatum. Insect molecular biology, 26(4), 414–419. https://doi.org/10.1111/imb.12304

17. Budachetri, K., Kumar, D., Crispell, G. et al. The tick endosymbiont Candidatus Midichloria mitochondrii and selenoproteins are essential for the growth of Rickettsia parkeri in the Gulf Coast tick vector. Microbiome 6, 141 (2018). https://doi.org/10.1186/s40168-018-0524-2

18. Callahan, B. J., McMurdie, P. J., Rosen, M. J., Han, A. W., Johnson, A. J., & Holmes, S. P. (2016). DADA2: High-resolution sample inference from Illumina amplicon data. Nature methods, 13(7), 581–583. https://doi.org/10.1038/nmeth.3869

19. Chong, J.; Liu, P.; Zhou, G.; Xia, J. Using Microbiome Analyst for comprehensive statistical, functional, and meta-analysis of microbiome data. Nat. Protoc. 2020, 15, 799–821

20. Chow C-ET, Kim DY, Sachdeva R, Caron DA, Fuhrman JA. Top-down controls on bacterial community structure: microbial network analysis of bacteria, T4-like viruses and protists. ISME J. 2014;8(4):816–29. https://doi.org/10.1038/ismej.2013.199.

21. Couper, L. I., Kwan, J. Y., Ma, J., & Swei, A. (2019). Drivers and patterns of microbial community assembly in a Lyme disease vector. Ecology and evolution, 9(13), 7768–7779. https://doi.org/10.1002/ece3.5361

22. Crispell, G., Budachetri, K., & Karim, S. (2016). Rickettsia parkeri colonization in Amblyomma maculatum: the role of superoxide dismutases. Parasites & vectors, 9(1), 291. https://doi.org/10.1186/s13071-016-1579-1

23. Dastgheyb, S. S., & Otto, M. (2015). Staphylococcal adaptation to diverse physiologic niches: an overview of transcriptomic and phenotypic changes in different biological environments. Future microbiology, 10(12), 1981–1995. https://doi.org/10.2217/fmb.15.116

24. de la Fuente, J., Antunes, S., Bonnet, S., Cabezas-Cruz, A., Domingos, A. G., Estrada-Peña, A., Johnson, N., Kocan, K. M., Mansfield, K. L., Nijhof, A. M., Papa, A., Rudenko, N., Villar, M., Alberdi, P., Torina, A., Ayllón, N., Vancova, M., Golovchenko, M., Grubhoffer, L., Caracappa, S., … Rego, R. (2017). Tick-

Pathogen Interactions and Vector Competence: Identification of Molecular Drivers for Tick-Borne Diseases. Frontiers in cellular and infection microbiology, 7, 114. https://doi.org/10.3389/fcimb.2017.00114

25. de la Fuente, J., Villar, M., Cabezas-Cruz, A., Estrada-Peña, A., Ayllón, N., & Alberdi, P. (2016). Tick-Host-Pathogen Interactions: Conflict and Cooperation. PLoS pathogens, 12(4), e1005488. https://doi.org/10.1371/journal.ppat.1005488

26. Deepak Kumar, Surendra Raj Sharma, Abdulsalam Adegoke et al. Recently evolved Francisella-like endosymbiont outcompetes an ancient and evolutionarily associated Coxiella-like endosymbiont in the lone star tick (Amblyomma americanum) linked to the Alpha-Gal Syndrome, 03 September 2021, PREPRINT (Version 1) available at Research Square [https://doi.org/10.21203/rs.3.rs-856007/v1]

27. Dhariwal, A.; Chong, J.; Habib, S.; King, I.L.; Agellon, L.B.; Xia, J. Microbiome Analyst: A web-based tool for comprehensive statistical, visual and meta-analysis of microbiome data. Nucleic Acids Res. 2017, 45, W180–W188.

28. Duron, O., Binetruy, F., Noël, V., Cremaschi, J., McCoy, K. D., Arnathau, C., et al. (2017). Evolutionary changes in symbiont community structure in ticks. *Mol. Ecol.* 26, 2905–2921. doi:10.1111/mec.14094.

29. Duron, O., Morel, O., Noël, V., Buysse, M., Binetruy, F., Lancelot, R., Loire, E., Ménard, C., Bouchez, O., Vavre, F., & Vial, L. (2018). Tick-Bacteria Mutualism Depends on B Vitamin Synthesis Pathways. Current biology : CB, 28(12), 1896–1902.e5. https://doi.org/10.1016/j.cub.2018.04.038

30. Eiler A, Heinrich F, Bertilsson S. Coherent dynamics and association networks among lake bacterioplankton taxa. ISME J. 2012;6(2):330–42.

31. Fiorotti, J., Menna-Barreto, R., Gôlo, P. S., Coutinho-Rodrigues, C., Bitencourt, R., Spadacci-Morena, D. D., Angelo, I., & Bittencourt, V. (2019). Ultrastructural and Cytotoxic Effects of Metarhizium robertsii Infection on Rhipicephalus microplus Hemocytes. Frontiers in physiology, 10, 654. https://doi.org/10.3389/fphys.2019.00654

32. Fogaça, A. C., Sousa, G., Pavanelo, D. B., Esteves, E., Martins, L. A., Urbanová, V., Kopáček, P., & Daffre, S. (2021). Tick Immune System: What Is Known, the

Interconnections, the Gaps, and the Challenges. Frontiers in immunology, 12, 628054. https://doi.org/10.3389/fimmu.2021.628054

33. Franta, Z., Frantová, H., Konvičková, J. et al. Dynamics of digestive proteolytic system during blood feeding of the hard tick Ixodes ricinus. Parasites Vectors 3, 119 (2010). https://doi.org/10.1186/1756-3305-3-119

34. Friedman, J., & Alm, E. J. (2012). Inferring correlation networks from genomic survey data. PLoS computational biology, 8(9), e1002687. https://doi.org/10.1371/journal.pcbi.1002687

35. Fröhlich E. (2002). Aufbau und Funktion von Blut-Gewebe-Schranken [Structure and function of blood-tissue barriers]. Deutsche medizinische Wochenschrift (1946), 127(49), 2629–2634. https://doi.org/10.1055/s-2002-35932

36. Gaio, A.d.O., Gusmão, D.S., Santos, A.V. et al. Contribution of midgut bacteria to blood digestion and egg production in Aedes aegypti (diptera: culicidae) (L.). Parasites Vectors 4, 105 (2011). https://doi.org/10.1186/1756-3305-4-105

37. Gil, J. C., Helal, Z. H., Risatti, G., & Hird, S. M. (2020). Ixodes scapularis microbiome correlates with life stage, not the presence of human pathogens, in ticks submitted for diagnostic testing. PeerJ, 8, e10424. https://doi.org/10.7717/peerj.10424

38. Gottlieb, Y., Lalzar, I., & Klasson, L. (2015). Distinctive genome reduction rates revealed by genomic analyses of two *Coxiella*-like endosymbionts in ticks. *Genome Biology and Evolution*, *7*(6), 1779–1796. https ://doi.org/10.1093/gbe/evv108

39. Greay, T. L., Gofton, A. W., Paparini, A., Ryan, U. M., Oskam, C. L., & Irwin, P. J. (2018). Recent insights into the tick microbiome gained through next-generation sequencing. Parasites & vectors, 11(1), 12. https://doi.org/10.1186/s13071-017-2550-5

40. Guizzo, M. G., Parizi, L. F., Nunes, R. D., Schama, R., Albano, R. M., Tirloni, L., et al. (2017). A Coxiella mutualist symbiont is essential to the development of Rhipicephalus microplus. *Sci. Rep.* 7, 17554. doi:10.1038/s41598-017-17309-x.

41. Guizzo, M. G., Neupane, S., Kucera, M., Perner, J., Frantová, H., da Silva Vaz, I., de Oliveira, P. L., Kopacek, P., & Zurek, L. (2020). Poor Unstable Midgut

Microbiome of Hard Ticks Contrasts With Abundant and Stable Monospecific Microbiome in Ovaries. Frontiers in cellular and infection microbiology, 10, 211. https://doi.org/10.3389/fcimb.2020.00211

42. Hillyer, J. F., & Strand, M. R. (2014). Mosquito hemocyte-mediated immune responses. Current opinion in insect science, 3, 14–21. https://doi.org/10.1016/j.cois.2014.07.002

43. Hillyer, J.F. Transcription in mosquito hemocytes in response to pathogen exposure. J Biol 8, 51 (2009). https://doi.org/10.1186/jbiol151

44. Houk, E.J. (1977).Midgut ultrastructure of Culex tarsalis (Diptera: Culcidae) before and after a bloodmeal Tissue and Cell, 9 (1) (1977), pp. 103-118

45. Hoxmeier, J. C., Fleshman, A. C., Broeckling, C. D., Prenni, J. E., Dolan, M. C., Gage, K. L., & Eisen, L. (2017). Metabolomics of the tick-Borrelia interaction during the nymphal tick blood meal. Scientific reports, 7, 44394. https://doi.org/10.1038/srep44394

46. Hunter, D. J., Torkelson, J. L., Bodnar, J., Mortazavi, B., Laurent, T., Deason, J., … Zhong, J. (2015). The *Rickettsia* endosymbiont of *Ixodes pacificus* contains all the genes of de novo folate biosynthesis. *PLoS ONE*, *10*(12), e0144552. e0144552https ://doi.org/10.1371/journal.pone.0144552

47. K. Kadota, S. Walter, F. G. Claveria, I. Igarashi, D. Taylor, K. Fujisaki, Morphological and Populational Characteristics of Hemocytes of Ornithodoros moubata Nymphs During the Ecdysial Phase , Journal of Medical Entomology, Volume 40, Issue 6, 1 November 2003, Pages 770–776, https://doi.org/10.1603/0022-2585-40.6.770

48. Jing, TZ., Qi, FH. & Wang, ZY. Most dominant roles of insect gut bacteria: digestion, detoxification, or essential nutrient provision?. Microbiome 8, 38 (2020). https://doi.org/10.1186/s40168-020-00823

49. Karim, S., Budachetri, K., Mukherjee, N., Williams, J., Kausar, A., Hassan, M. J., Adamson, S., Dowd, S. E., Apanskevich, D., Arijo, A., Sindhu, Z. U., Kakar, M. A., Khan, R., Ullah, S., Sajid, M. S., Ali, A., & Iqbal, Z. (2017). A study of ticks and tick-borne livestock pathogens in Pakistan. PLoS neglected tropical diseases, 11(6), e0005681. https://doi.org/10.1371/journal.pntd.0005681

50. King, J.G., Hillyer, J.F. Spatial and temporal in vivo analysis of circulating and sessile immune cells in mosquitoes: hemocyte mitosis following infection. BMC Biol 11, 55 (2013). https://doi.org/10.1186/1741-7007-11-55

51. Kueneman, J. G., Esser, H. J., Weiss, S. J., Jansen, P. A., & Foley, J. E. (2021). Tick Microbiomes in Neotropical Forest Fragments Are Best Explained by Tick-Associated and Environmental Factors Rather than Host Blood Source. Applied and environmental microbiology, 87(7), e02668-20. https://doi.org/10.1128/AEM.02668-20

52. Kumar, D., Budachetri, K., Meyers, V. C., & Karim, S. (2016). Assessment of tick antioxidant responses to exogenous oxidative stressors and insight into the role of catalase in the reproductive fitness of the Gulf Coast tick, Amblyomma maculatum. Insect molecular biology, 25(3), 283–294. https://doi.org/10.1111/imb.12218

53. Kurokawa, C., Lynn, G.E., Pedra, J.H.F. et al. Interactions between Borrelia burgdorferi and ticks. Nat Rev Microbiol 18, 587–600 (2020). https://doi.org/10.1038/s41579-020-0400-5

54. Kwon, H., & Smith, R. C. (2019). Chemical depletion of phagocytic immune cells in Anopheles gambiae reveals dual roles of mosquito hemocytes in anti-Plasmodium immunity. Proceedings of the National Academy of Sciences of the United States of America, 116(28), 14119–14128. https://doi.org/10.1073/pnas.1900147116

55. Landesman, W. J., Mulder, K., Allan, B. F., Bashor, L. A., Keesing, F., LoGiudice, K., & Ostfeld, R. S. (2019). Potential effects of blood meal host on bacterial community composition in Ixodes scapularis nymphs. Ticks and tick-borne diseases, 10(3), 523–527. https://doi.org/10.1016/j.ttbdis.2019.01.002

56. Lejal, E., Moutailler, S., Šimo, L. et al. Tick-borne pathogen detection in midgut and salivary glands of adult Ixodes ricinus. Parasites Vectors 12, 152 (2019). https://doi.org/10.1186/s13071-019-3418-7

57. Liu, L., Cheng, T. Y., & He, X. M. (2018). Proteomic profiling of the midgut contents of Haemaphysalis flava. Ticks and tick-borne diseases, 9(3), 490–495. https://doi.org/10.1016/j.ttbdis.2018.01.008

58. Liu, L., Narasimhan, S., Dai, J., Zhang, L., Cheng, G., & Fikrig, E. (2011). Ixodes scapularis salivary gland protein P11 facilitates migration of Anaplasma phagocytophilum from the tick gut to salivary glands. EMBO reports, 12(11), 1196–1203. https://doi.org/10.1038/embor.2011.177

59. Lopatkin, A. J., & Yang, J. H. (2021). Digital Insights Into Nucleotide Metabolism and Antibiotic Treatment Failure. Frontiers in digital health, 3, 583468. https://doi.org/10.3389/fdgth.2021.583468

60. Maldonado-Ruiz, L.P., Neupane, S., Park, Y. et al. The bacterial community of the lone star tick (Amblyomma americanum). Parasites Vectors 14, 49 (2021). https://doi.org/10.1186/s13071-020-04550-z

61. Mann AE, Mitchell EA, Zhang Y, Curtis-Robles R, Thapa S, Hamer SA, et al. comparison of the bacterial gut microbiome of North American Triatoma spp. with and without Trypanosoma cruzi. Front Microbiol. 2020;11. doi:10.3389/fmicb.2020.00364.

62. Microsoft Corporation. (2018). Microsoft Excel. Retrieved from https://office.microsoft.com/excel

63. Mukhacheva, T. A., & Kovalev, S. Y. (2017). Bacteria of the Family 'Candidatus Midichloriaceae' in Sympatric Zones of Ixodes Ticks: Genetic Evidence for Vertical Transmission. Microbial ecology, 74(1), 185–193. https://doi.org/10.1007/s00248-017-0932-z

64. Muturi, E. J., Dunlap, C., Ramirez, J. L., Rooney, A. P., & Kim, C. H. (2019). Host blood-meal source has a strong impact on gut microbiota of Aedes aegypti. FEMS microbiology ecology, 95(1), 10.1093/femsec/fiy213. https://doi.org/10.1093/femsec/fiy213

65. Narasimhan, S., & Fikrig, E. (2015). Tick microbiome: the force within. Trends in parasitology, 31(7), 315–323. https://doi.org/10.1016/j.pt.2015.03.010

66. Narasimhan, S., Swei, A., Abouneameh, S., Pal, U., Pedra, J., & Fikrig, E. (2021). Grappling with the tick microbiome. Trends in parasitology, 37(8), 722–733. https://doi.org/10.1016/j.pt.2021.04.004

67. Nuttall P. A. (2019). Tick saliva and its role in pathogen transmission. Wiener klinische Wochenschrift, 10.1007/s00508-019-1500-y. Advance online publication. https://doi.org/10.1007/s00508-019-1500-y

68. Nuttall, P., & Labuda, M. (2008). Saliva-assisted transmission of tick-borne pathogens. In A. Bowman & P. Nuttall (Eds.), Ticks: Biology, Disease and Control (pp. 205-219). Cambridge: Cambridge University Press. doi:10.1017/CBO9780511551802.011

69. Obregón, D., Bard, E., Abrial, D., Estrada-Peña, A., & Cabezas-Cruz, A. (2019). Sex-Specific Linkages Between Taxonomic and Functional Profiles of Tick Gut Microbiomes. Frontiers in cellular and infection microbiology, 9, 298. https://doi.org/10.3389/fcimb.2019.00298

70. Oleaga, A., Obolo-Mvoulouga, P., Manzano-Román, R. et al. A proteomic insight into the midgut proteome of Ornithodoros moubata females reveals novel information on blood digestion in argasid ticks. Parasites Vectors 10, 366 (2017). https://doi.org/10.1186/s13071-017-2300-8

71. Oliveira JL, Cury JC, Gurgel-Gonçalves R, Bahia AC, Monteiro FA. Field-collected Triatoma sordida from central Brazil display high microbiota diversity that varies with regard to developmental stage and intestinal segmentation. PLoS Negl Trop Dis. 2018;12:e0006709.

72. Olivieri, E., Epis, S., Castelli, M., Varotto Boccazzi, I., Romeo, C., Desirò, A., … Sassera, D. (2019). Tissue tropism and metabolic pathways of *Midichloria mitochondrii* suggest tissue-specific functions in the symbiosis with *Ixodes ricinus*. *Ticks and Tick-Borne Diseases*, *10*(5), 1070–1077. https ://doi.org/10.1016/j.ttbdis.2019.05.019

73. Onyango, L. A., & Alreshidi, M. M. (2018). Adaptive Metabolism in Staphylococci: Survival and Persistence in Environmental and Clinical Settings. Journal of pathogens, 2018, 1092632. https://doi.org/10.1155/2018/1092632

74. Paddock CD, Goddard J. The evolving medical and veterinary importance of the Gulf Coast tick (Acari: Ixodidae). J Med Entomol. 2015;52:230–52.Return to ref 2 in article

75. Patrick CD, Hair JA. Laboratory rearing procedures and equipment for multi-host ticks (Acarina: Ixodidae). J Med Entomol. 1975;12:389–90.

76. Pereira, L. S., Oliveira, P. L., Barja-Fidalgo, C., & Daffre, S. (2001). Production of reactive oxygen species by hemocytes from the cattle tick Boophilus microplus. Experimental parasitology, 99(2), 66–72. https://doi.org/10.1006/expr.2001.4657

77. Perner, J., Provazník, J., Schrenková, J. et al. RNA-seq analyses of the midgut from blood- and serum-fed Ixodes ricinus ticks. Sci Rep 6, 36695 (2016). https://doi.org/10.1038/srep36695

78. Philipp Engel, Nancy A. Moran, The gut microbiota of insects – diversity in structure and function, FEMS Microbiology Reviews, Volume 37, Issue 5, September 2013, Pages 699–735, https://doi.org/10.1111/1574-6976.12025

79. Pollet T, Sprong H, Lejal E, Krawczyk AI, Moutailler S, Cosson J-F, et al. The scale affects our view on the identification and distribution of microbial communities in ticks. Parasit Vectors. 2020;13(1):36. https://doi.org/10.1186/s13071-020-3908-7.

80. Ponnusamy, L., Gonzalez, A., Van Treuren, W., Weiss, S., Parobek, C. M., Juliano, J. J., Knight, R., Roe, R. M., Apperson, C. S., & Meshnick, S. R. (2014). Diversity of Rickettsiales in the microbiome of the lone star tick, Amblyomma americanum. Applied and environmental microbiology, 80(1), 354–359. https://doi.org/10.1128/AEM.02987-13

81. Portillo, A., Palomar, A. M., de Toro, M., Santibáñez, S., Santibáñez, P., & Oteo, J. A. (2019). Exploring the bacteriome in anthropophilic ticks: To investigate the vectors for diagnosis. PloS one, 14(3), e0213384. https://doi.org/10.1371/journal.pone.0213384

82. Powers, J. C., Turangan, R., Joosse, B. A., & Hillyer, J. F. (2020). Adult Mosquitoes Infected with Bacteria Early in Life Have Stronger Antimicrobial Responses and More Hemocytes after Reinfection Later in Life. Insects, 11(6), 331. https://doi.org/10.3390/insects11060331

83. Quast C, Pruesse E, Yilmaz P, Gerken J, Schweer T, Yarza P, Peplies J, Glöckner FO (2013) The SILVA ribosomal RNA gene database project: improved data processing and web-based tools. Opens external link in new windowNucl. Acids Res. 41 (D1): D590-D596.

84. Rachinsky, A., Guerrero, F. D., & Scoles, G. A. (2008). Proteomic profiling of Rhipicephalus (Boophilus) microplus midgut responses to infection with Babesia bovis. Veterinary parasitology, 152(3-4), 294–313. https://doi.org/10.1016/j.vetpar.2007.12.027

85. Ravine TJ. Bacillus: An Environmental Contaminant or Misunderstood Pathogen?. J Bacteriol Mycol. 2019; 6(6): 1117.

86. Ribeiro, J. M., Zeidner, N. S., Ledin, K., Dolan, M. C., & Mather, T. N. (2004). How much pilocarpine contaminates pilocarpine-induced tick saliva?. Medical and veterinary entomology, 18(1), 20–24. https://doi.org/10.1111/j.0269-283x.2003.0469.

87. Rojas-Jaimes, J., Lindo-Seminario, D., Correa-Núñez, G. et al. Characterization of the bacterial microbiome of Rhipicephalus (Boophilus) microplus collected from Pecari tajacu "Sajino" Madre de Dios, Peru. Sci Rep 11, 6661 (2021). https://doi.org/10.1038/s41598-021-86177-3

88. Ross, A.A., Rodrigues Hoffmann, A. & Neufeld, J.D. The skin microbiome of vertebrates. Microbiome 7, 79 (2019). https://doi.org/10.1186/s40168-019-0694-6

89. Ross, B. D., Hayes, B., Radey, M. C., Lee, X., Josek, T., Bjork, J., Neitzel, D., Paskewitz, S., Chou, S., & Mougous, J. D. (2018). Ixodes scapularis does not harbor a stable midgut microbiome. The ISME journal, 12(11), 2596–2607. https://doi.org/10.1038/s41396-018-0161-6

90. Schwarz, A., Tenzer, S., Hackenberg, M., Erhart, J., Gerhold-Ay, A., Mazur, J., Kuharev, J., Ribeiro, J. M., & Kotsyfakis, M. (2014). A systems level analysis reveals transcriptomic and proteomic complexity in Ixodes ricinus midgut and salivary glands during early attachment and feeding. Molecular & cellular proteomics : MCP, 13(10), 2725–2735. https://doi.org/10.1074/mcp.M114.039289

91. Sigle, L. T., & Hillyer, J. F. (2016). Mosquito hemocytes preferentially aggregate and phagocytose pathogens in the periostial regions of the heart that experience the most hemolymph flow. Developmental and comparative immunology, 55, 90–101. https://doi.org/10.1016/j.dci.2015.10.018

92. Sigle, L. T., & Hillyer, J. F. (2018). Mosquito Hemocytes Associate With Circulatory Structures That Support Intracardiac Retrograde Hemolymph Flow. Frontiers in physiology, 9, 1187. https://doi.org/10.3389/fphys.2018.01187

93. Šimo, L., Kazimirova, M., Richardson, J., & Bonnet, S. I. (2017). The Essential Role of Tick Salivary Glands and Saliva in Tick Feeding and Pathogen Transmission. Frontiers in cellular and infection microbiology, 7, 281. https://doi.org/10.3389/fcimb.2017.00281

94. Smith, T. A., Driscoll, T., Gillespie, J. J., & Raghavan, R. (2015). A Coxiella-like endosymbiont is a potential vitamin source for the Lone Star tick. Genome biology and evolution, 7(3), 831–838. https://doi.org/10.1093/gbe/evv016

95. Sonenshine D. E. (2018). Range Expansion of Tick Disease Vectors in North America: Implications for Spread of Tick-Borne Disease. International journal of environmental research and public health, 15(3), 478. https://doi.org/10.3390/ijerph15030478

96. Starck, J.M., Mehnert, L., Biging, A. et al. Morphological responses to feeding in ticks (Ixodes ricinus). Zoological Lett 4, 20 (2018). https://doi.org/10.1186/s40851-018-0104-0

97. Swei, A., Kwan, J. Tick microbiome and pathogen acquisition altered by host blood meal. ISME J 11, 813–816 (2017). https://doi.org/10.1038/ismej.2016.152

98. Tarnowski, B. I., & Coons, L. B. (1989). Ultrastructure of the midgut and blood meal digestion in the adult tick Dermacentor variabilis. Experimental & applied acarology, 6(4), 263–289. https://doi.org/10.1007/BF01193300

99. Thapa, S., Zhang, Y. & Allen, M.S. Bacterial microbiomes of Ixodes scapularis ticks collected from Massachusetts and Texas, USA. BMC Microbiol 19, 138 (2019). https://doi.org/10.1186/s12866-019-1514-7

100. Thapa, S., Zhang, Y., & Allen, M. S. (2019). Effects of temperature on bacterial microbiome composition in Ixodes scapularis ticks. MicrobiologyOpen, 8(5), e00719. https://doi.org/10.1002/mbo3.719

101. Tirloni, L., Braz, G., Nunes, R.D. et al. A physiologic overview of the organ-specific transcriptome of the cattle tick Rhipicephalus microplus. Sci Rep 10, 18296 (2020). https://doi.org/10.1038/s41598-020-75341-w

102.   Trappeniers, K., Matetovici, I., Van Den Abbeele, J., & De Vooght, L. (2019). The Tsetse Fly Displays an Attenuated Immune Response to Its Secondary Symbiont, Sodalis glossinidius. Frontiers in microbiology, 10, 1650. https://doi.org/10.3389/fmicb.2019.01650

103.   Trout Fryxell, R. T., & DeBruyn, J. M. (2016). The Microbiome of Ehrlichia-Infected and Uninfected Lone Star Ticks (Amblyomma americanum). PloS one, 11(1), e0146651. https://doi.org/10.1371/journal.pone.0146651

104.   Valenzuela, J. G., Charlab, R., Mather, T. N., & Ribeiro, J. M. (2000). Purification, cloning, and expression of a novel salivary anticomplement protein from the tick, Ixodes scapularis. The Journal of biological chemistry, 275(25), 18717–18723. https://doi.org/10.1074/jbc.M001486200

105.   Varela-Stokes, A. S., Park, S. H., Stokes, J. V., Gavron, N. A., Lee, S. I., Moraru, G. M., & Ricke, S. C. (2018). Tick microbial communities within enriched extracts of Amblyomma maculatum. Ticks and tick-borne diseases, 9(4), 798–805. https://doi.org/10.1016/j.ttbdis.2018.02.022

106.   Wei, N., Cao, J., Zhang, H., Zhou, Y., & Zhou, J. (2021). The Tick Microbiota Dysbiosis Promote Tick-Borne Pathogen Transstadial Transmission in a Babesia microti-Infected Mouse Model. Frontiers in cellular and infection microbiology, 11, 713466. https://doi.org/10.3389/fcimb.2021.713466

107.   Wright, C. L., Gaff, H. D., Sonenshine, D. E., & Hynes, W. L. (2015). Experimental vertical transmission of Rickettsia parkeri in the Gulf Coast tick, Amblyomma maculatum. Ticks and tick-borne diseases, 6(5), 568–573. https://doi.org/10.1016/j.ttbdis.2015.04.011

108.   Zhang, X. C., Yang, Z. N., Lu, B., Ma, X. F., Zhang, C. X., & Xu, H. J. (2014). The composition and transmission of microbiome in hard tick, Ixodes persulcatus, during blood meal. Ticks and tick-borne diseases, 5(6), 864–870. https://doi.org/10.1016/j.ttbdis.2014.07.009

109.   Zhang, YK., Yu, ZJ., Wang, D. et al. The bacterial microbiome of field-collected Dermacentor marginatus and Dermacentor reticulatus from Slovakia. Parasites Vectors 12, 325 (2019). https://doi.org/10.1186/s13071-019-3582-9

1265   110.   Zhong, J., Jasinskas, A., & Barbour, A. G. (2007). Antibiotic treatment of the
1266   tick vector *Amblyomma americanum* reduced reproductive fitness. *PLoS ONE*,
1267   *2*(5), e405. https ://doi.org/10.1371/journal.pone.0000405

1268   111.   Zolnik, C. P., Falco, R. C., Daniels, T. J., & Kolokotronis, S. O. (2018).
1269   Transient influence of blood meal and natural environment on blacklegged tick
1270   bacterial communities. Ticks and tick-borne diseases, 9(3), 563–572.
1271   https://doi.org/10.1016/j.ttbdis.2018.01.007

1272   112.   Zolnik, C. P., Prill, R. J., Falco, R. C., Daniels, T. J., & Kolokotronis, S. O.
1273   (2016). Microbiome changes through ontogeny of a tick pathogen vector.
1274   Molecular ecology, 25(19), 4963–4977. https://doi.org/10.1111/mec.13832

1275

1276

1277

1278 **LIST OF FIGURES**
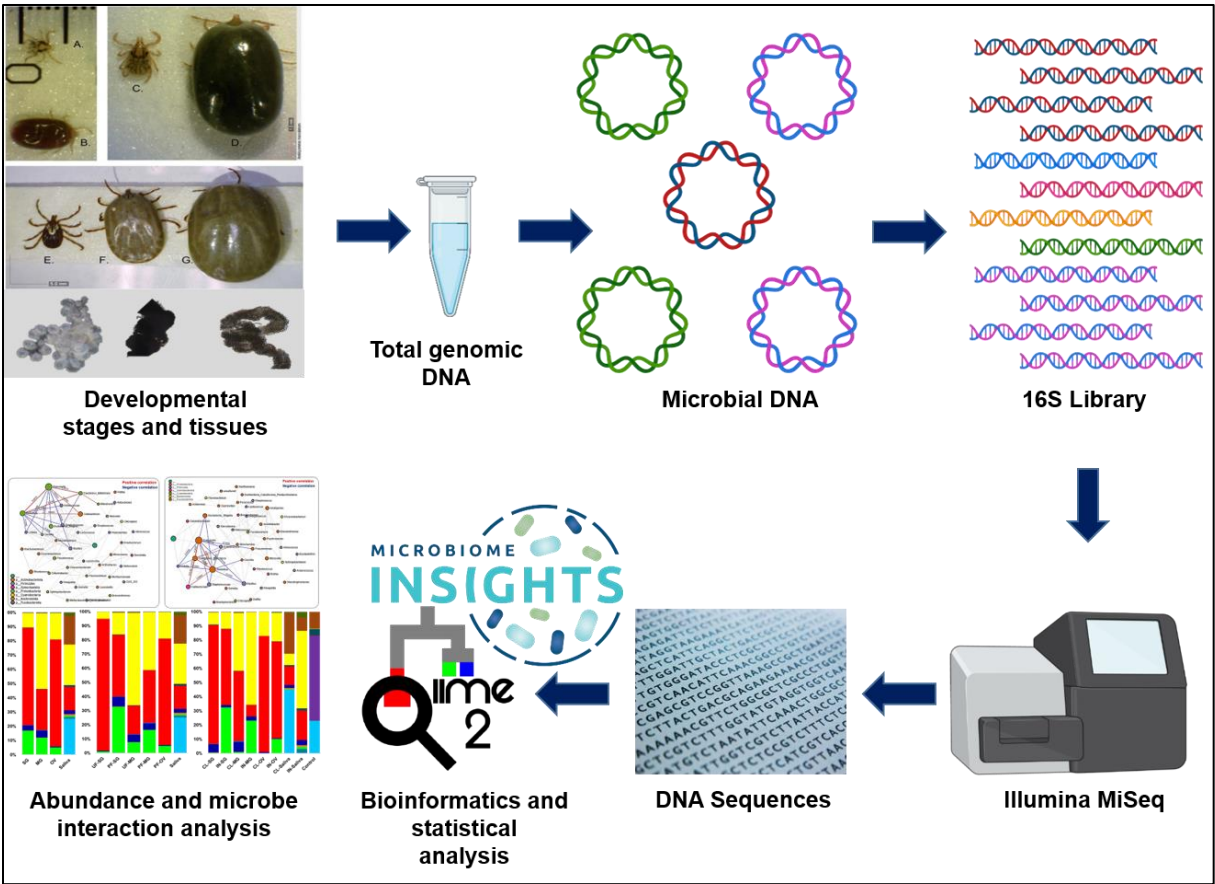
Graphical Abstract

1279

1280

1281

1282

1283

1284

1285

1286
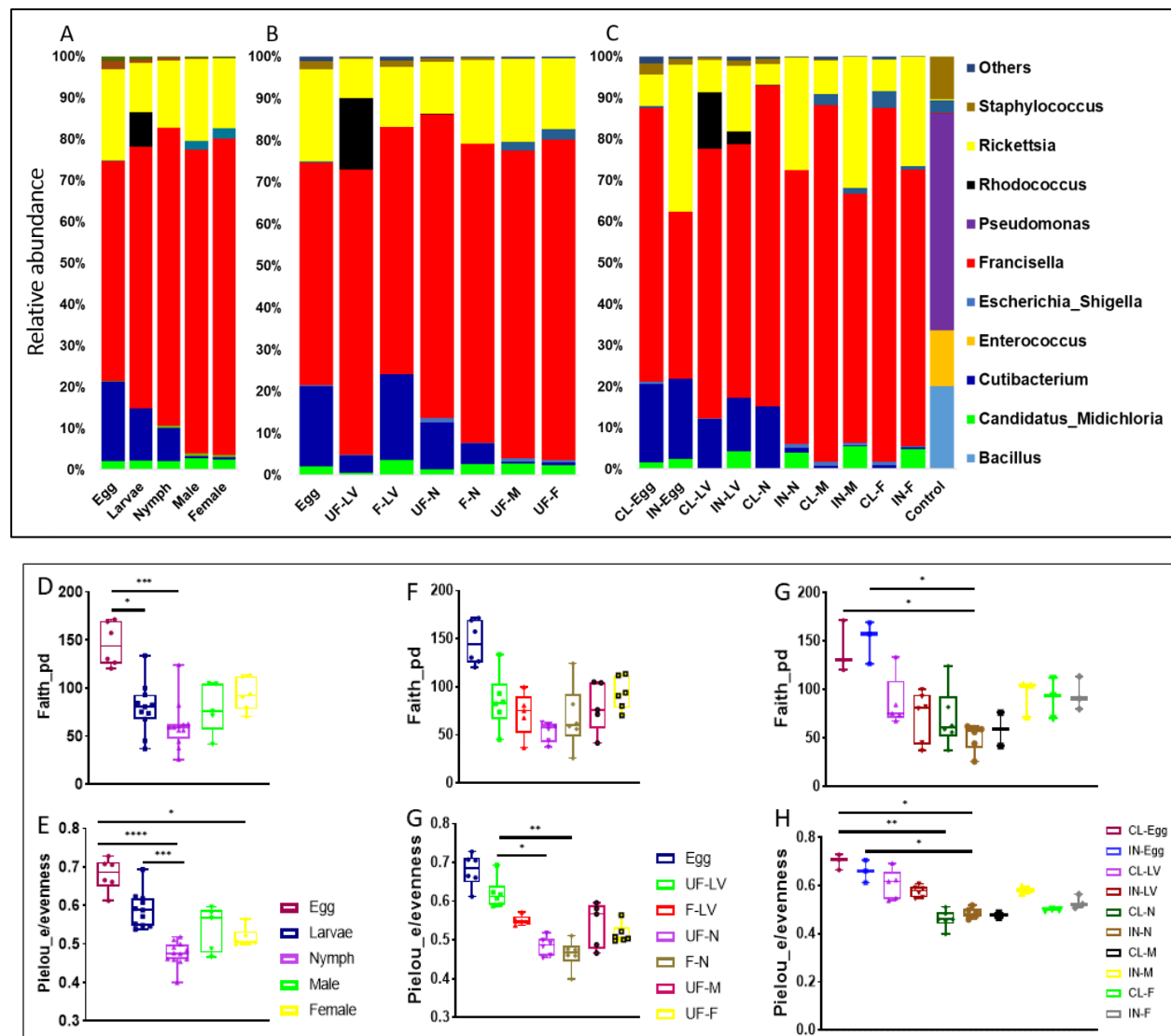
Figure 1: **Stability of bacterial abundances and microbial richness across developmental stages.** The relative abundances of the predominant members of microbial communities in A) all developmental stages, B) unfed and fully fed developmental stages and C) *R. parkeri*-infected and uninfected developmental stages. Diversity analysis using Faith phylogenetic distance (species richness) and Pielou_e metrics (evenness) in (D, E) all developmental stages, (F, G) unfed and fully fed developmental stages, and (H, I) *R. parkeri*-infected and uninfected developmental stages. Each bar on the abundance plot represents average data from 3–5 individual replicates. Each point of the box plots represents average data from 3–5 individual replicates. Unfed (UF), fed (F), larvae (LV), nymph (N), male (M), female (F), clean (CL), infected (IN).

1287

1288

1289

1290
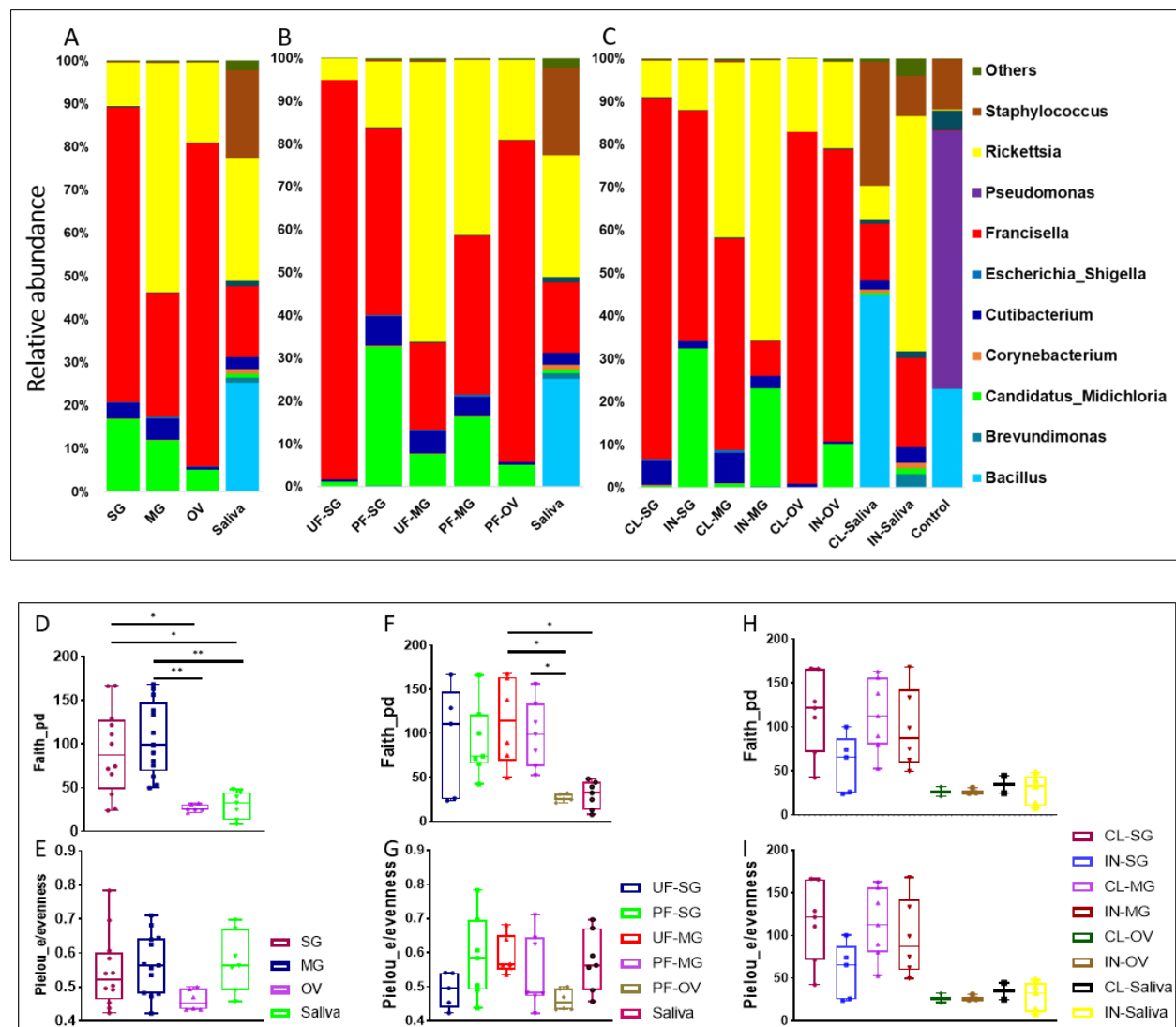
Figure 2: **Changes in microbial assemblages and diversity across different tissues.** The relative abundances of the predominant members of microbial communities in A) all isolated tissues, B) unfed and fully fed tissues, and C) *R. parkeri*-infected and uninfected tissues. Diversity analysis using Faith phylogenetic distance (specie richness) and Pielou_e metrics (evenness) in (D, E) all tissues, (F, G) unfed and fully fed tissues, and (H, I) *R. parkeri*-infected and uninfected tissues. Each bar on the abundance plot represents average data from 3–5 individual replicates. Each point of the box plots represents average data from 3–5 individual replicates. Unfed (UF), fed (F), larvae (LV), nymph (N), male (M), female (F), clean (CL), infected (IN). salivary gland (SG), midgut (MG), ovary (OV).
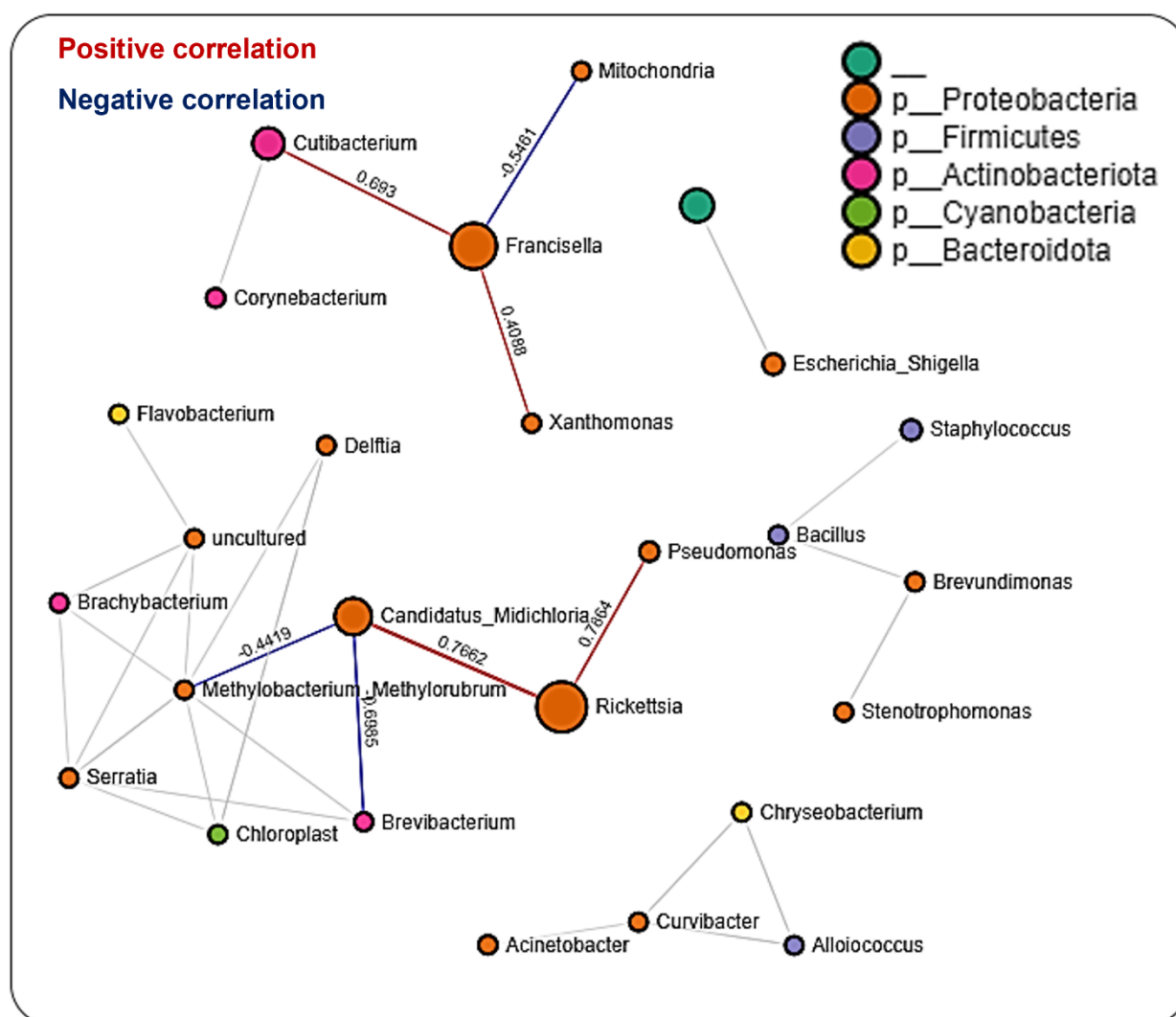
1291

1292

1293

1294

1295
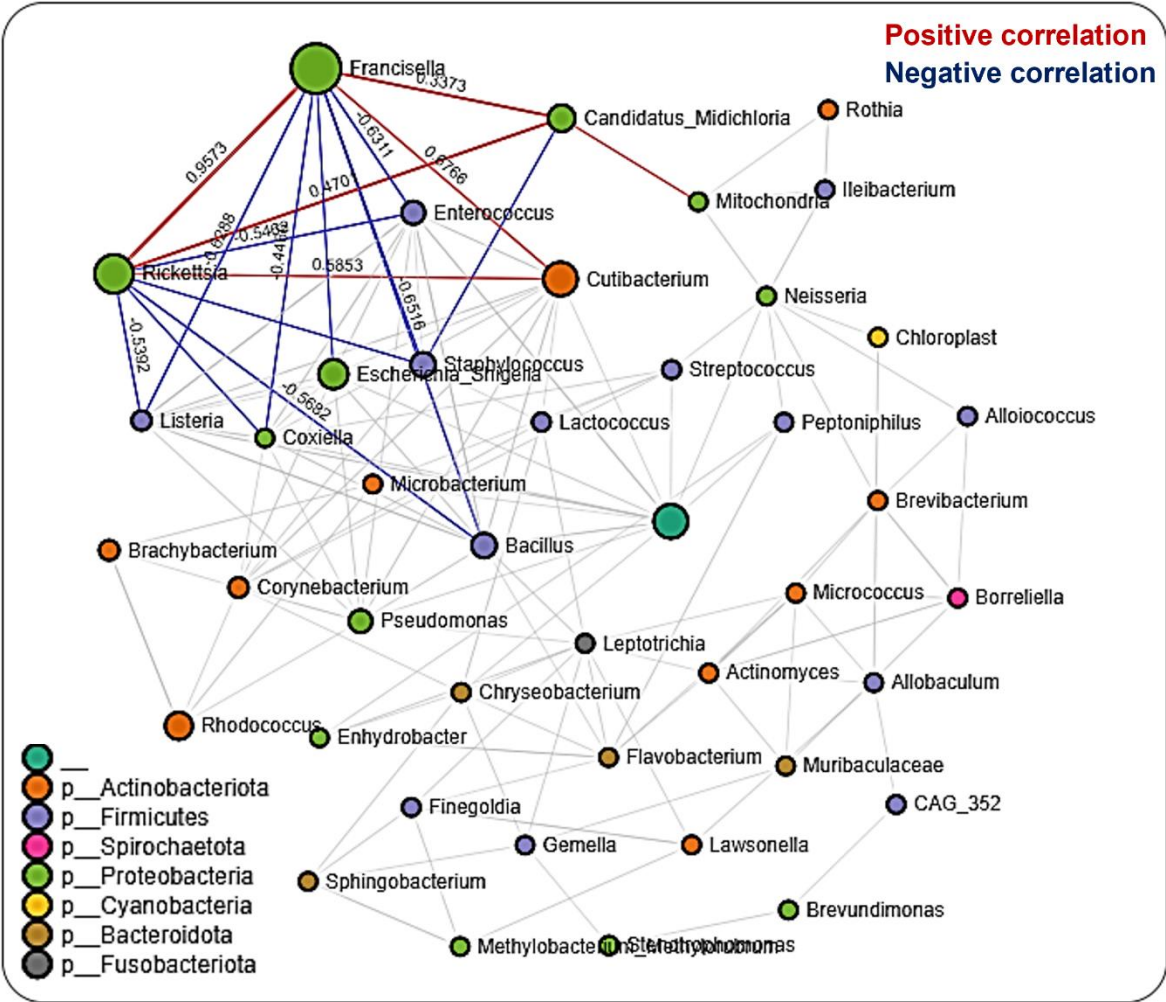
Figure 3: **Correlation network analysis across the life stages of *Am. maculatum* ticks**. Correlation network generated using the SparCC algorithm. Correlation network with nodes representing taxa at the family level and edges representing correlations between taxa pairs. Node size correlates with the number of interactions in which a taxon is involved, and the line color represents either positive (red) or negative (blue) correlations. The color-coded legend shows the bacterial family to which each taxon belongs.

1296

1297

1298

1299

1300

1301

1302

1303

Figure 4: Correlation network analysis across tissue stages of *Am. maculatum* ticks. Correlation network generated using the SparCC algorithm. Correlation network with nodes representing taxa at the family level and edges representing correlations between taxa pairs. Node size correlates with the number of interactions in which a taxon is involved, and the line color represents either positive (red) or negative (blue) correlations. The color-coded legend shows the bacterial family to which each taxon belongs.

1304

1305

1306

1307

1308

1309

1310
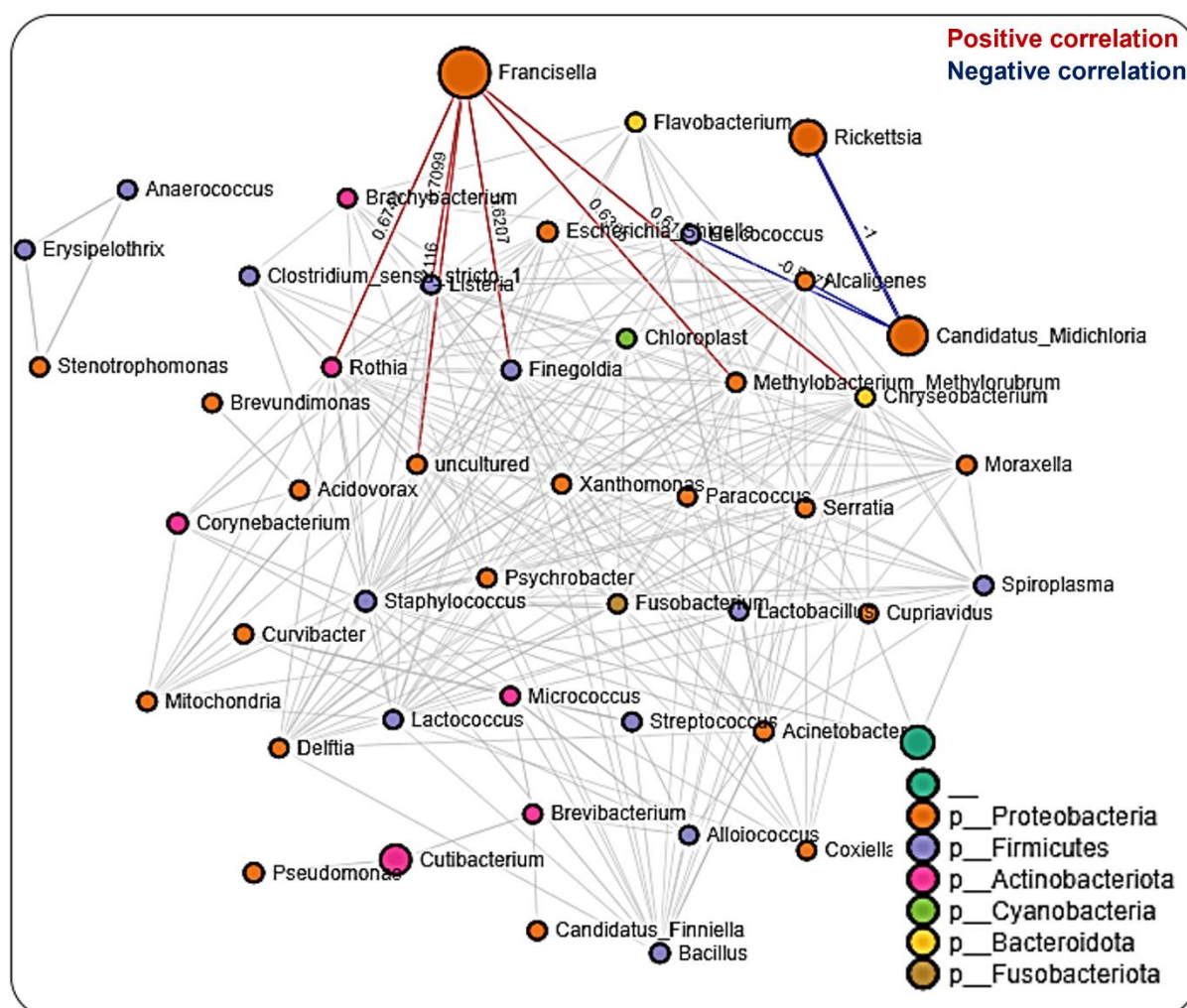
Figure 5: Correlation network analysis in the salivary glands of *Am. maculatum* ticks. Correlation network generated using the SparCC algorithm. Correlation network with nodes representing taxa at the family level and edges representing correlations between taxa pairs. Node size correlates with the number of interactions in which a taxon is involved, and the line color represents either positive (red) or negative (blue) correlations. The color-coded legend shows the bacterial family to which each taxon belongs.

1311

1312

1313

1314

1315

1316

1317

1318

Figure 6: Correlation network analysis in the midgut of *Am. maculatum* ticks. Correlation network generated using the SparCC algorithm. Correlation network with nodes representing taxa at the family level and edges representing correlations between taxa pairs. Node size correlates with the number of interactions in which a taxon is involved, and the line color represents either positive (red) or negative (blue) correlations. The color-coded legend shows the bacterial family to which each taxon belongs.

1319

1320

1321
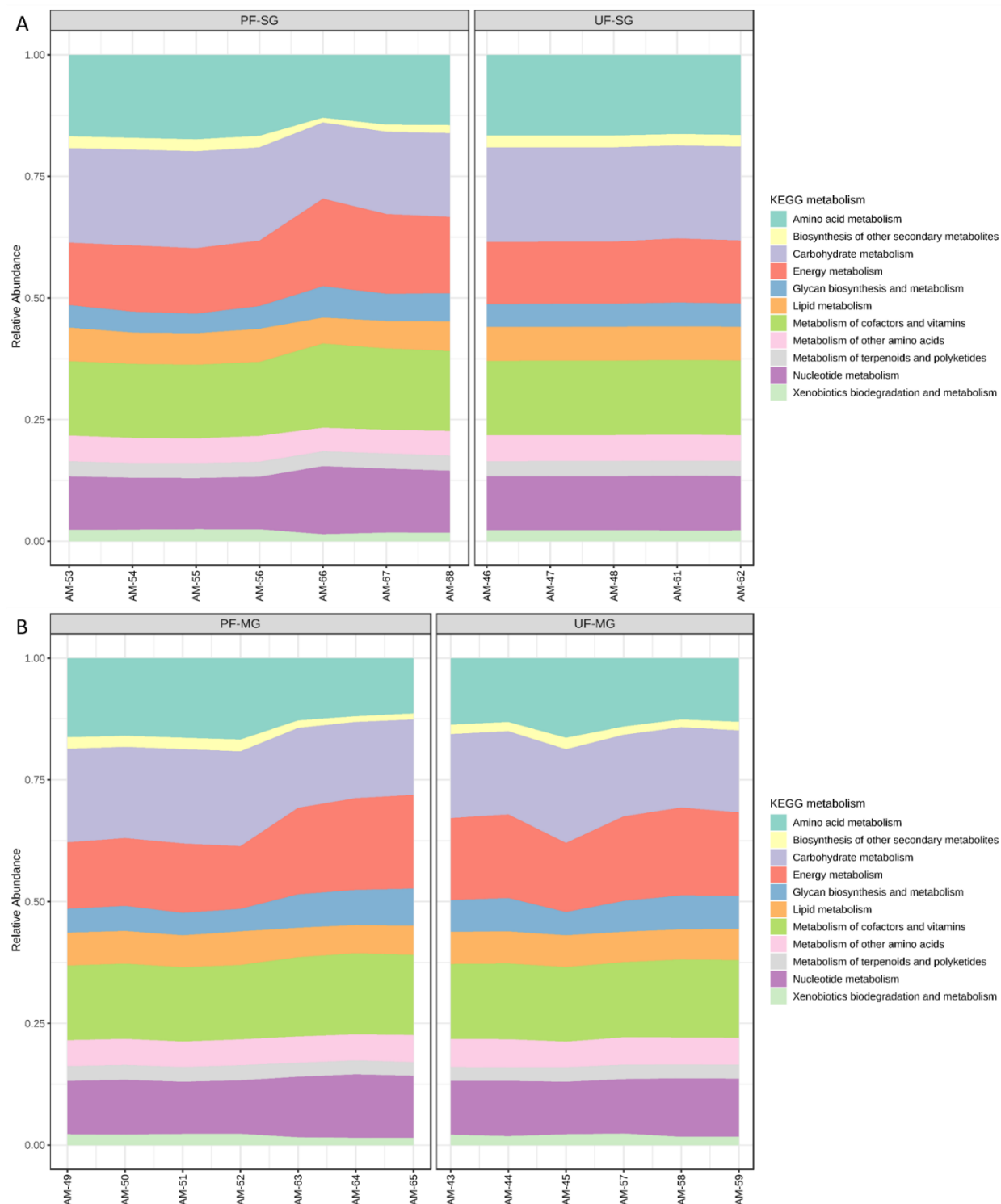
Figure 7: Histogram indicating the functional differences between the fed and partially fed Am. *maculatum* microbiota in A) salivary gland and B) midgut tissues. KEGG metabolic categories were obtained from 16S rRNA gene sequences using the PICRUSt2 pipeline.

1322

1323

1324
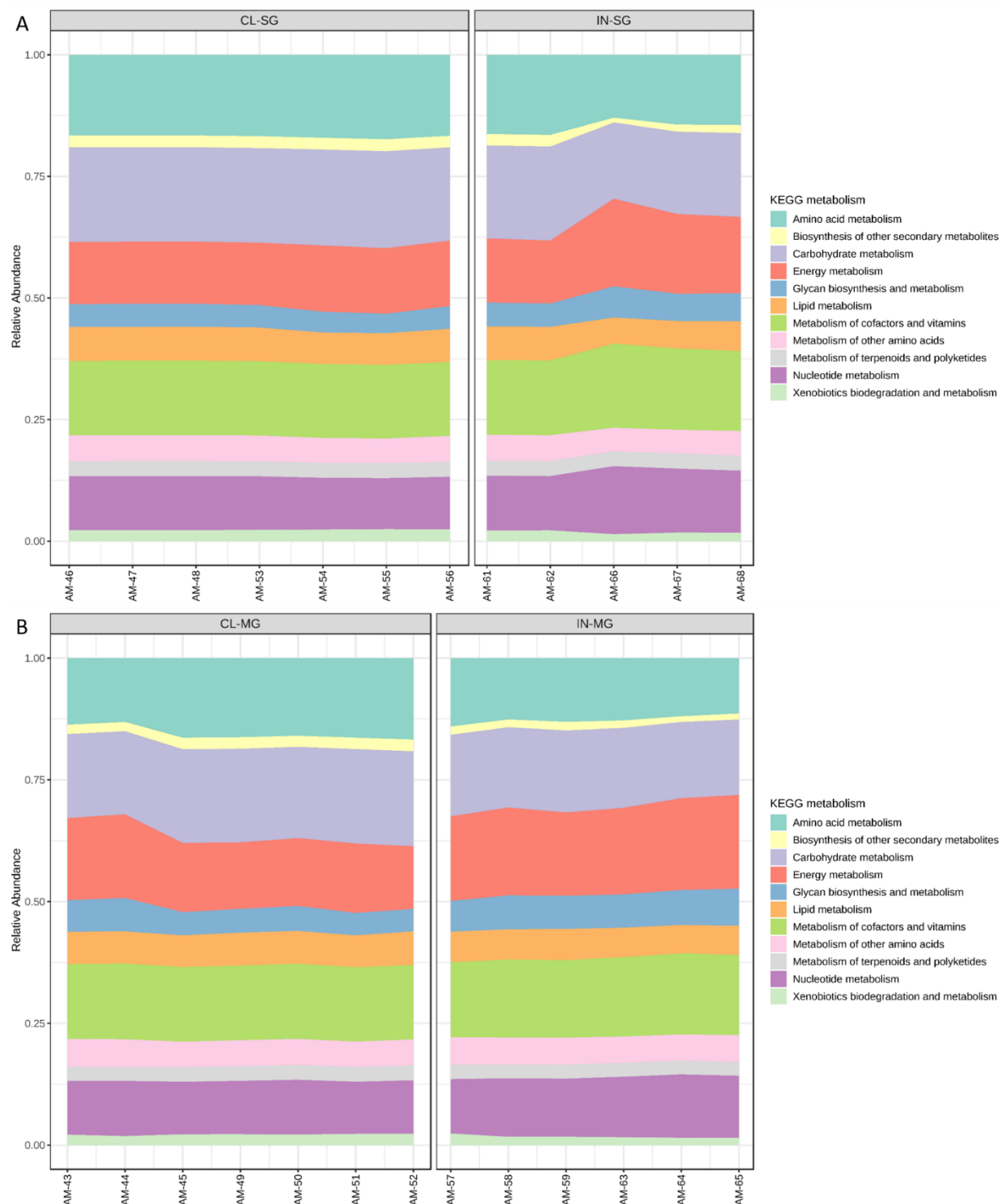
Figure 8: Histogram indicating the functional differences between the uninfected and *R. parkeri*-infected Am. *maculatum* microbiota in A) salivary gland and B) midgut tissues. KEGG metabolic categories were obtained from 16S rRNA gene sequences using the PICRUSt2 pipeline.

1325   **ADDITIONAL FILES**
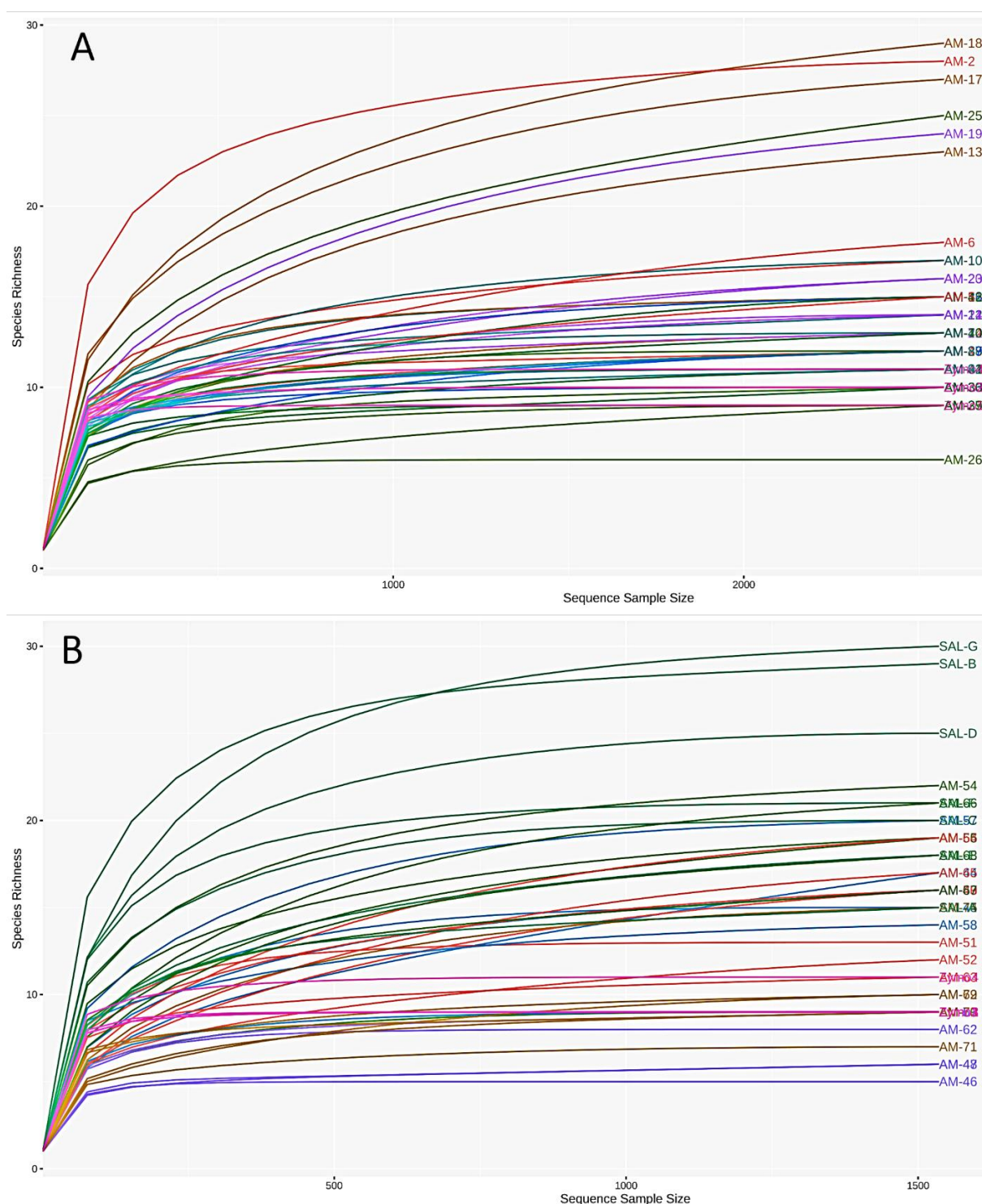
Figure S1: Rarefaction analysis of raw reads from A) developmental stages and B) isolated tissues of *Am. maculatum* ticks. Each curve representing individual replicates was rarified to a sequence depth of approximately 3000 sequences for all developmental stages (unfed and partially fed) and 1000 sequences for isolated tissues.

1326
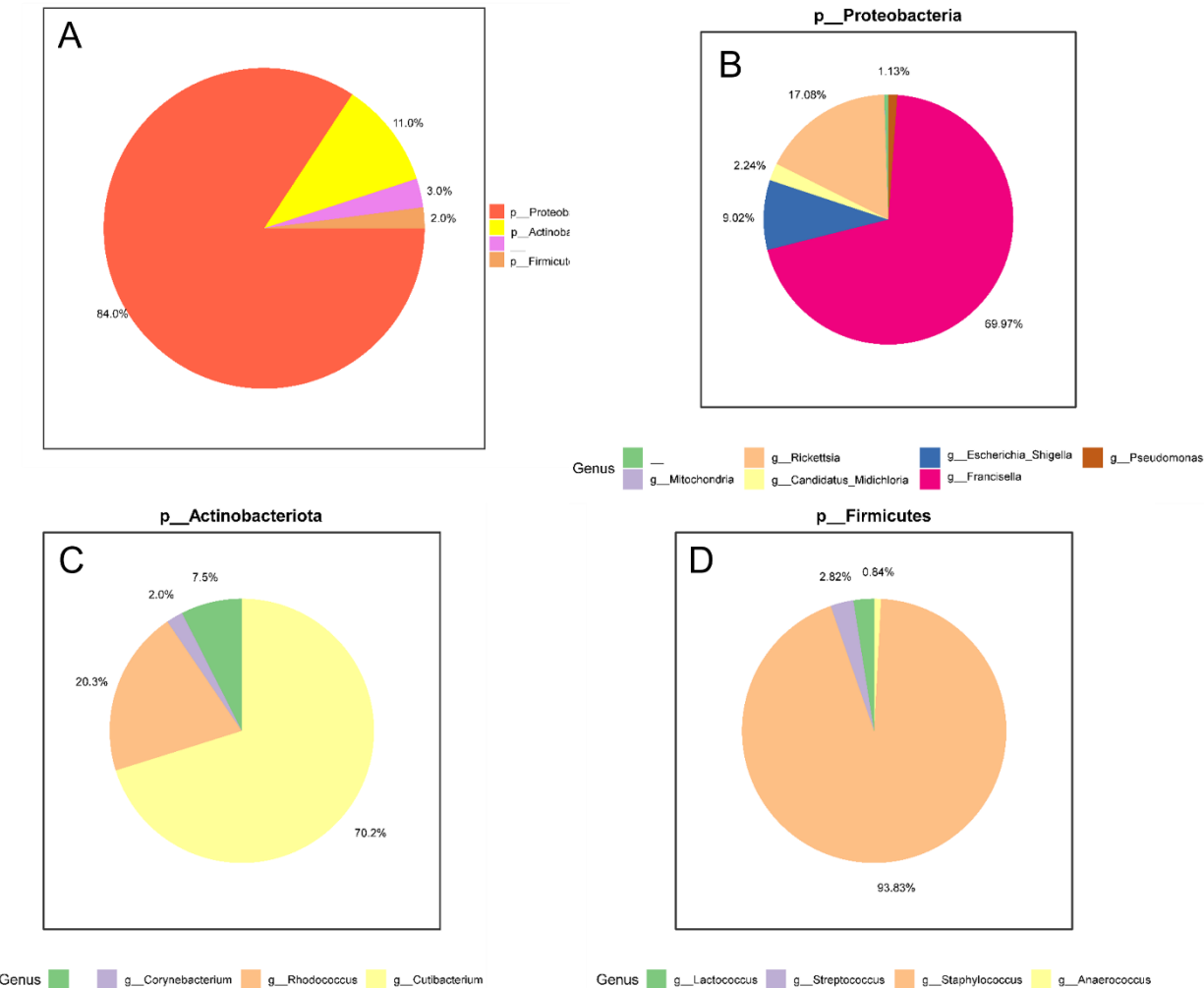
Figure S2: Pie chart summary of microbial abundances in the developmental stages of *Am. maculatum*. A) Overall abundance summary at the phylum taxonomic level and breakdown of abundant phyla showing B) Proteobacteria, C) Actinobacteriota, and D) Firmicutes. A representative genus from each phylum is indicated in the legends.

1327

1328

1329

1330

1331

1332

1333

1334

1335
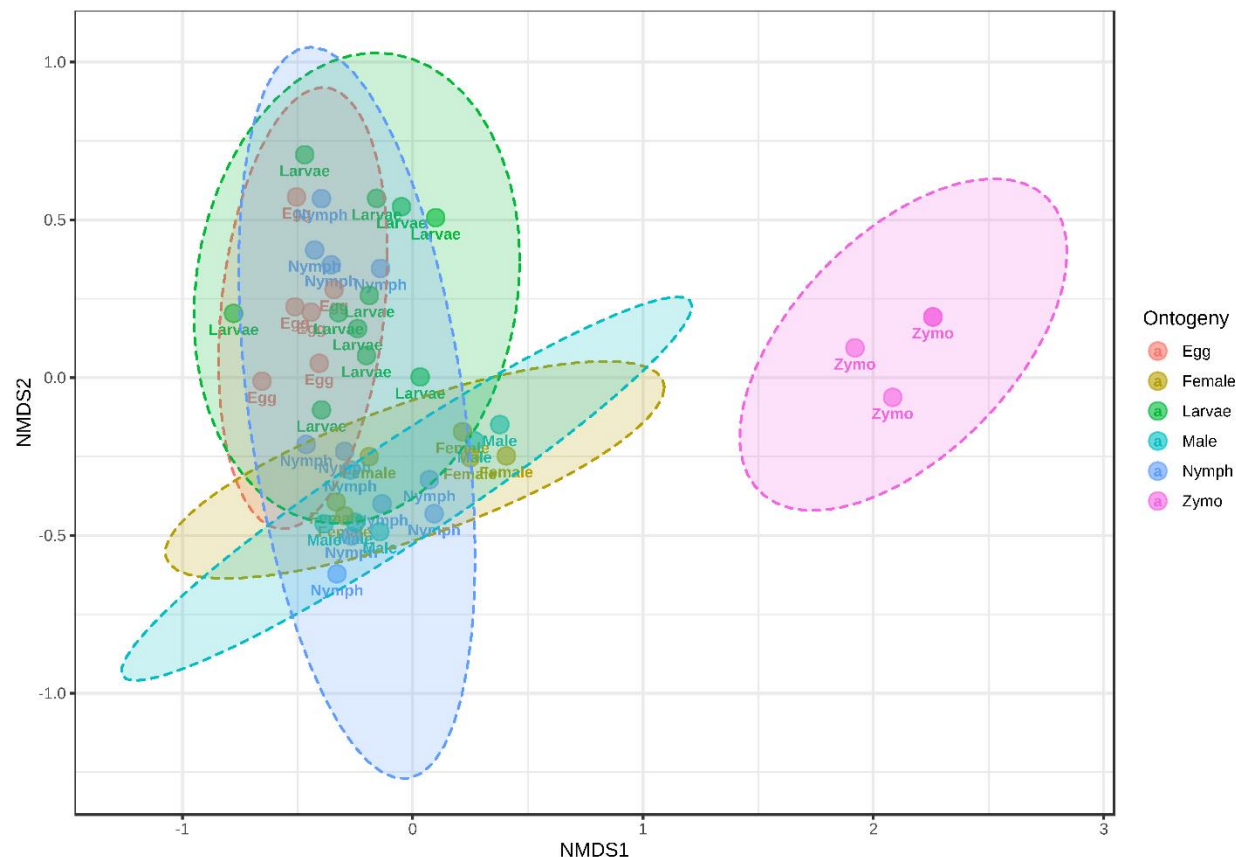
Figure S3: Non-metric multidimensional scaling (NMDA) analysis of β-diversity measures across *Am. maculatum* **developmental stages.** Ellipses around unique clusters indicate the degree of distance based on the Bray–Curtis distance matrix.

1336

1337
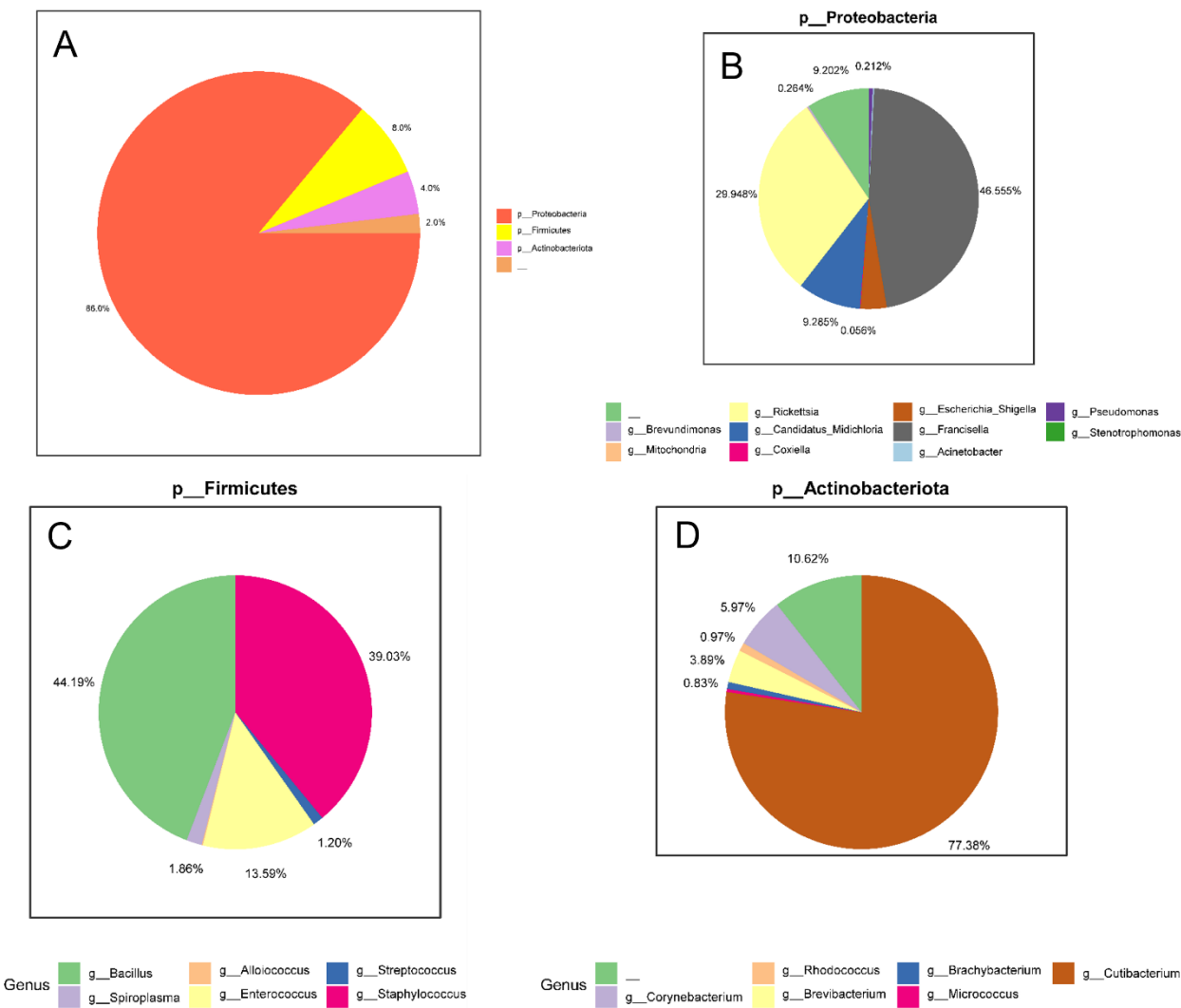
Figure S4: Pie chart summary of microbial abundances in the dissected tissues of *Am. maculatum.* A) Overall abundance summary at the phylum taxonomic level and breakdown of abundant phyla showing B) Proteobacteria, C) Firmicutes, and D) Actinobacteriota. A representative genus from each phylum is indicated in the legends.

1338

1339

1340

1341

1342

1343

1344

1345
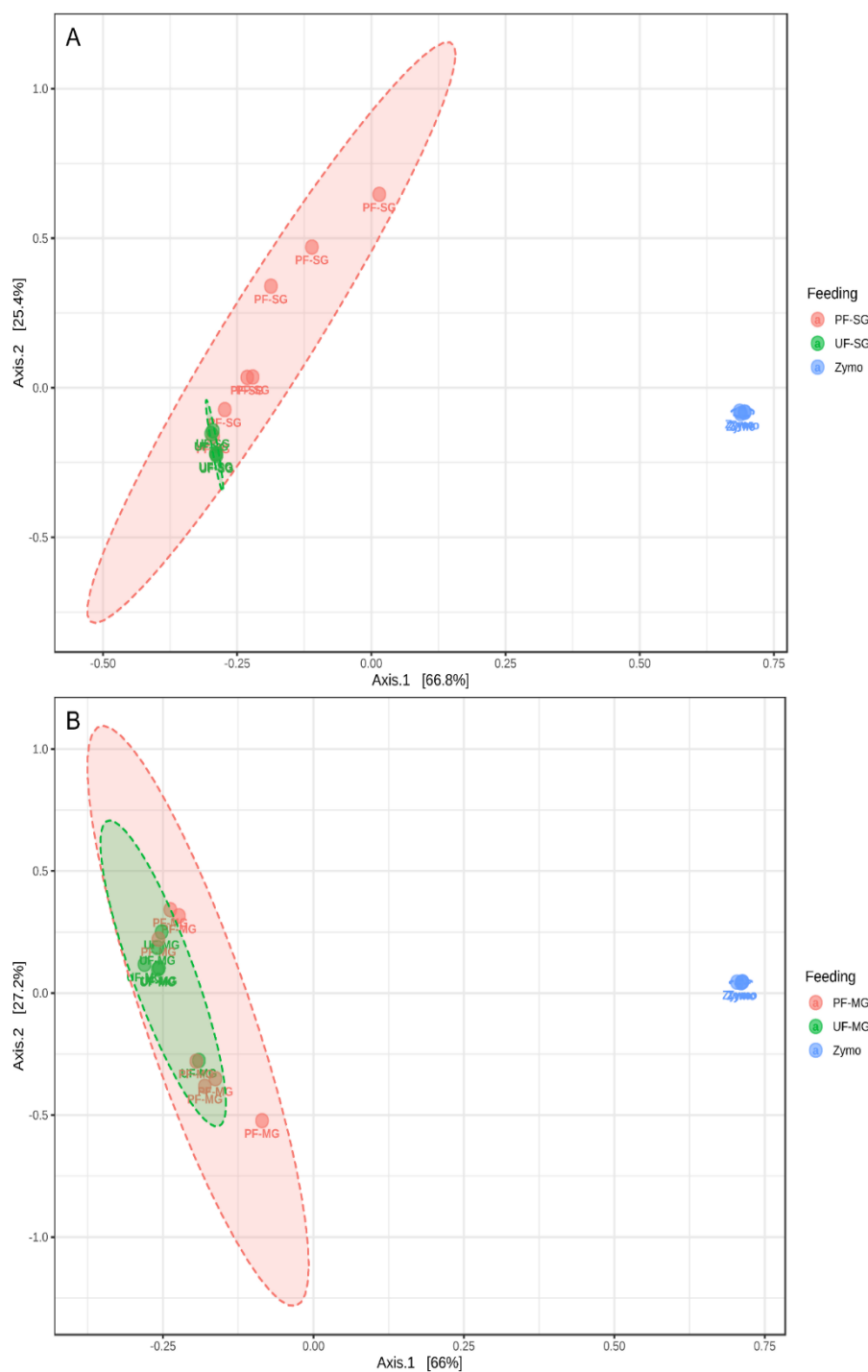
Figure S5: Principal coordinate analysis of β-diversity measures of tissues dissected from unfed and partially fed *Am. maculatum* ticks. Bray–Curtis distance matrix of A) salivary gland and B) midgut tissues. Ellipses around unique clusters indicate the degree of distance.

1346

1347
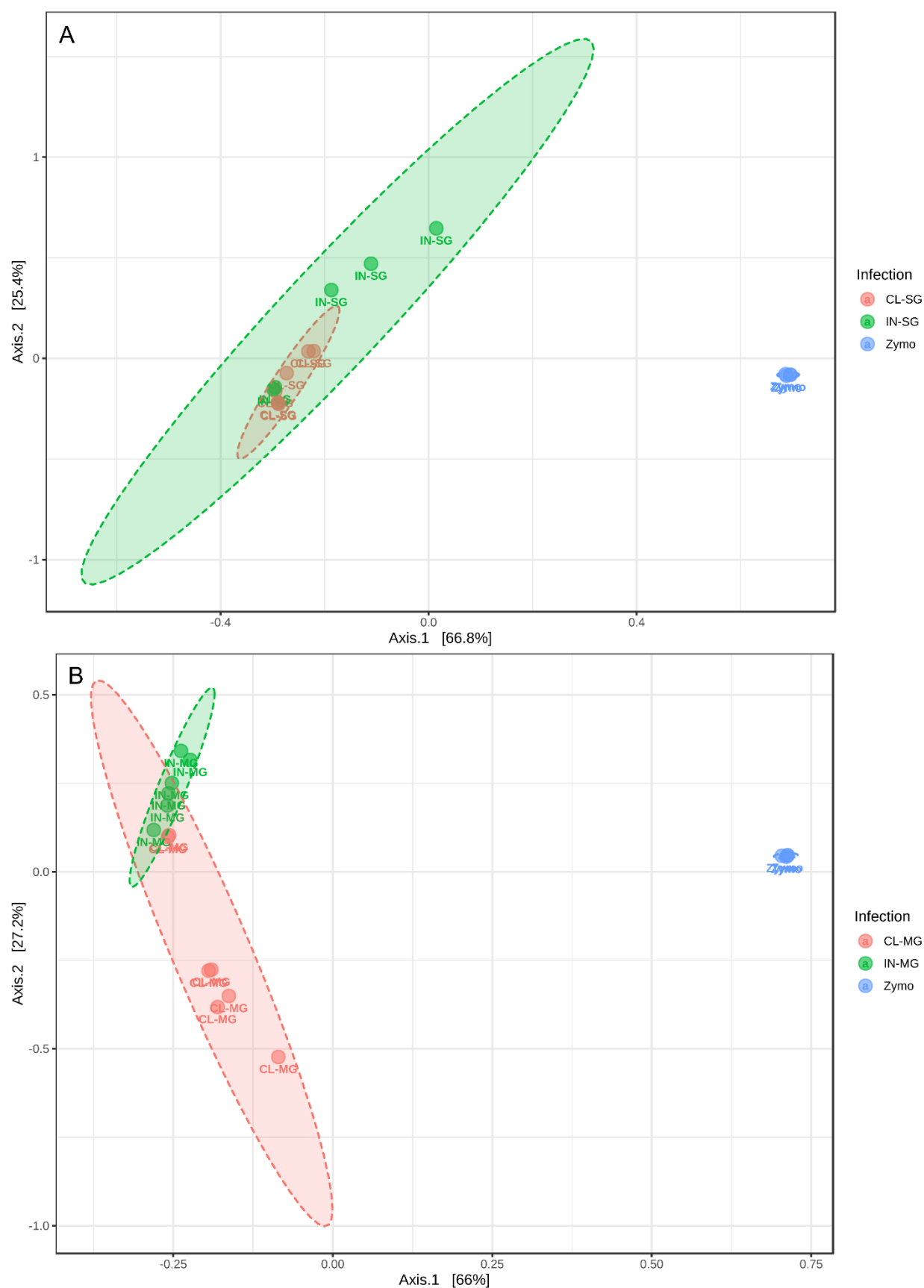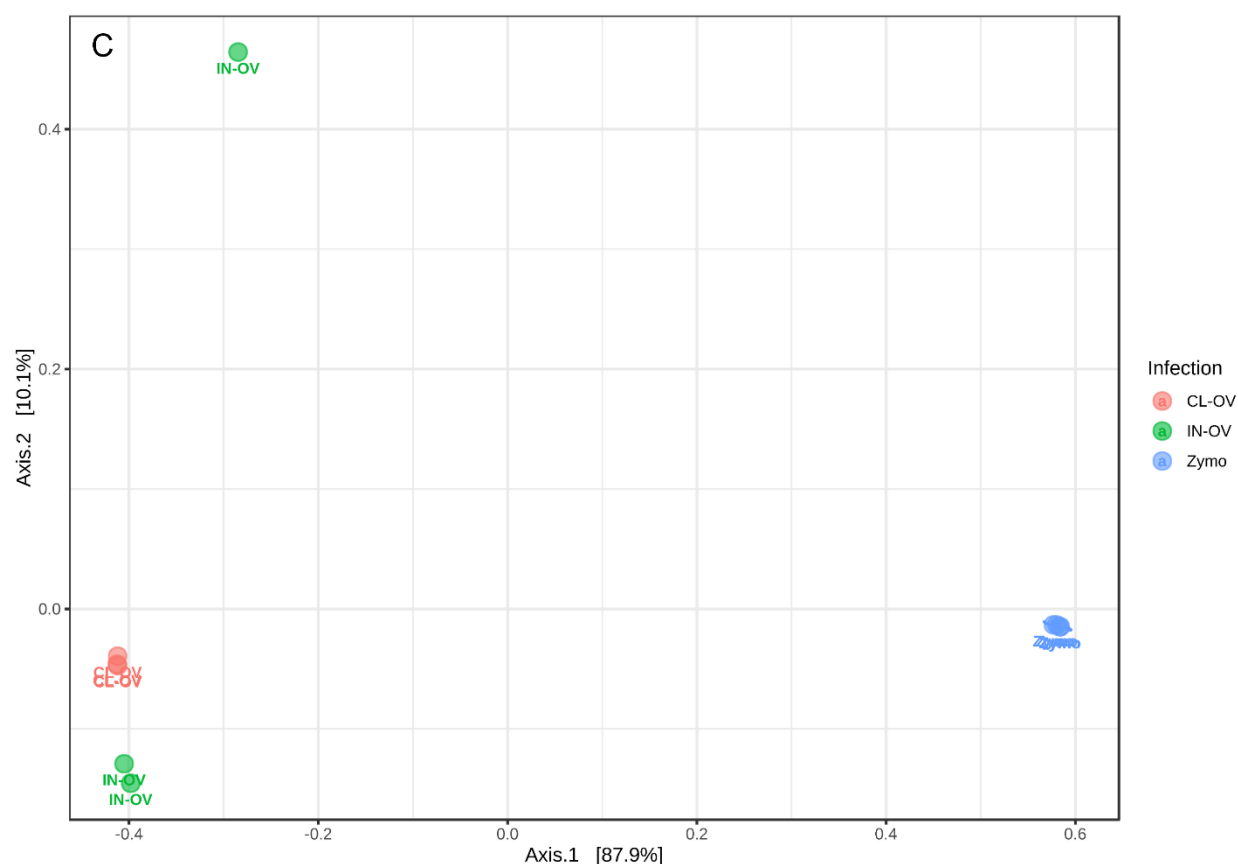
Figure S6: Principal coordinate analysis of β-diversity measures of tissues dissected from unfed and partially fed *Am. maculatum* ticks. Bray–Curtis distance matrix of A) salivary gland, B) midgut tissues, and C) ovarian tissues. Ellipses around unique clusters indicate the degree of distance.

1348

1349

1350

1351

1352

1353

1354

1355

1356

1357

1358
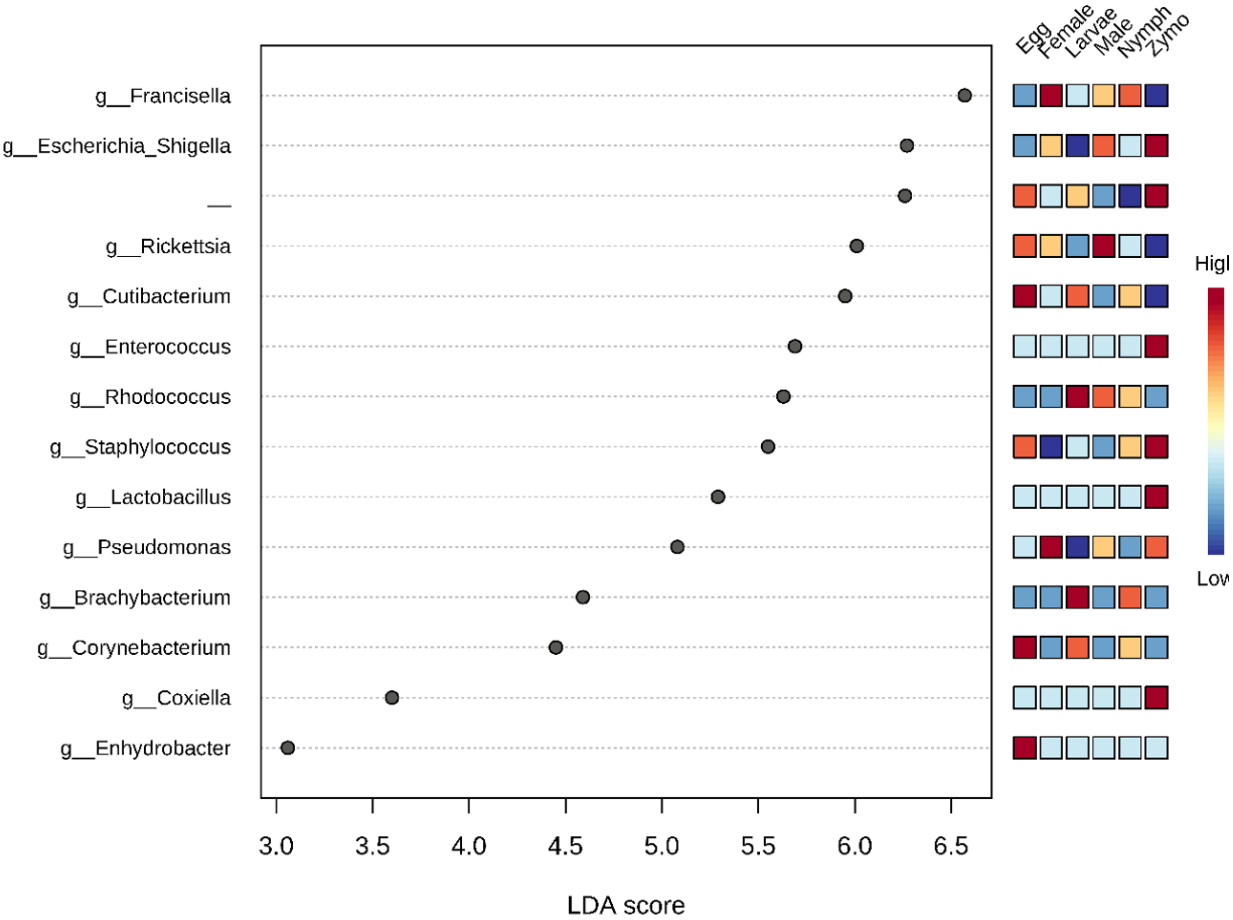
Figure S7: Graphical summary of LEfSe analysis across the developmental stages of *Am. maculatum*. Significant taxa are ranked in decreasing order by their LDA scores (x axis). The mini heat map to the right of the plot indicates whether the number of taxa are higher (red) or lower (blue) in each group.

1359
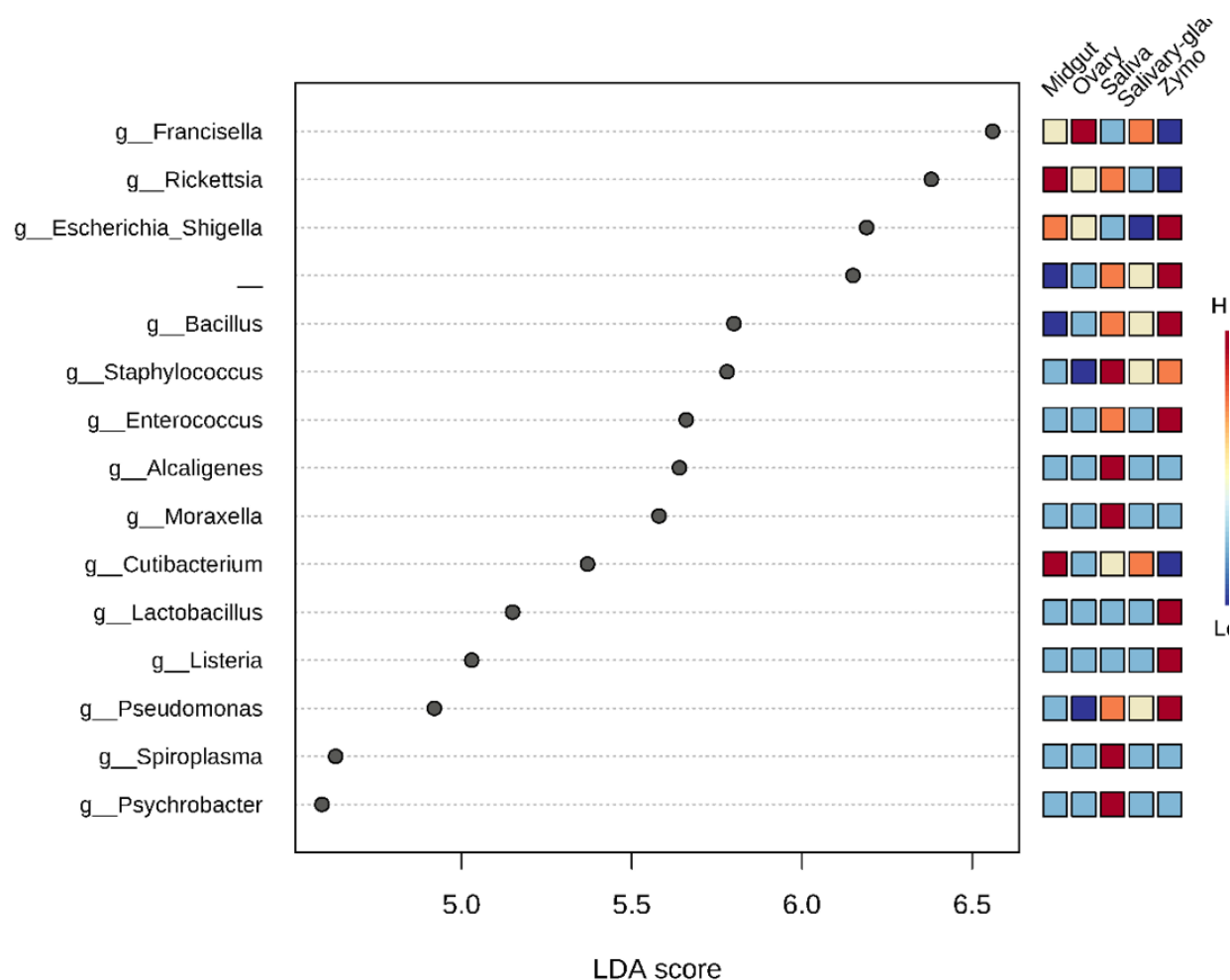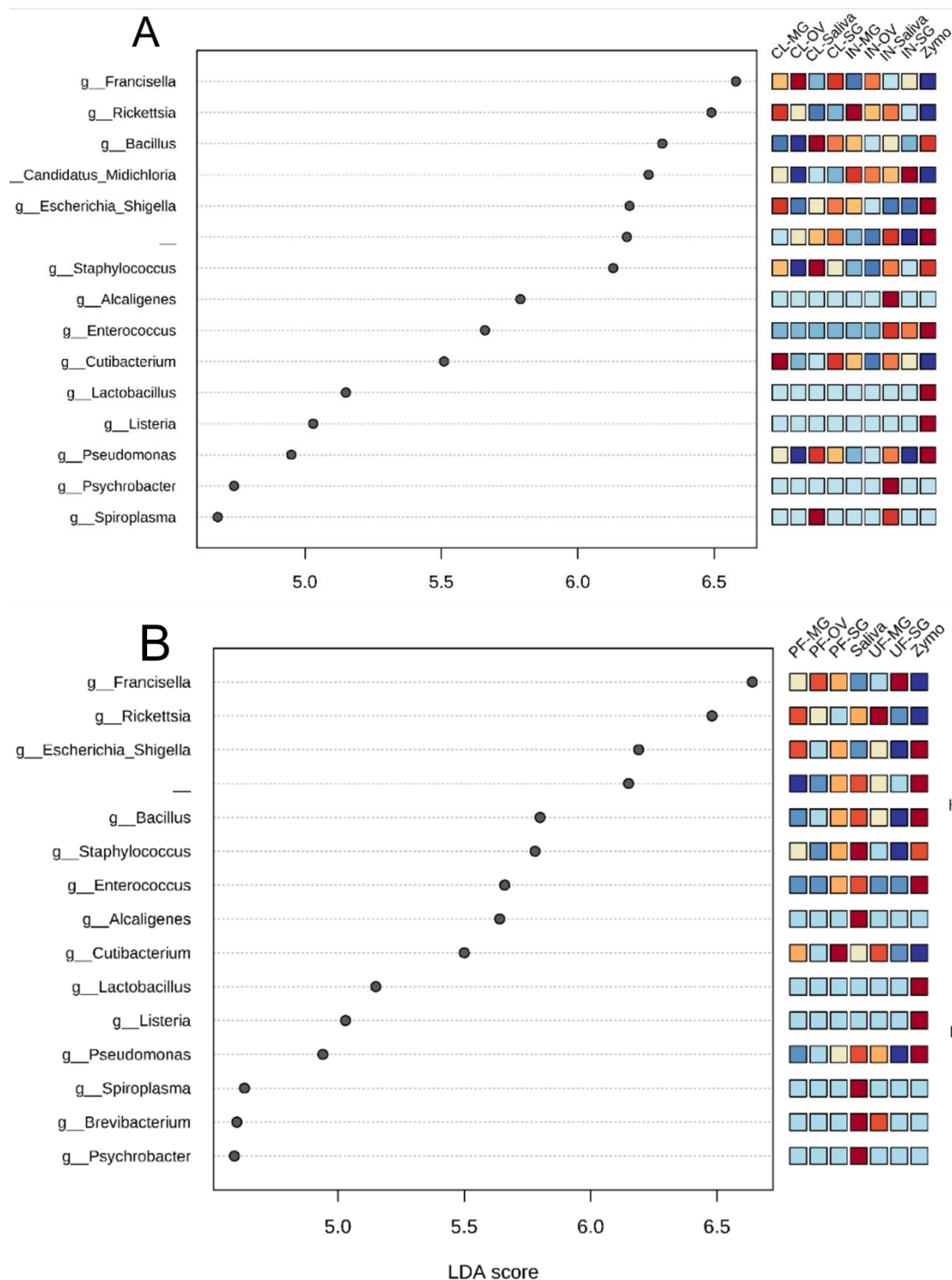
1360

1361

1362

1363

1364

1365

1366

Figure S8: Graphical summary of LEfSe analysis from the dissected tissues of *Am. maculatum*. Significant taxa are ranked in decreasing order by their LDA scores (x axis). The mini heat map to the right of the plot indicates whether the number of taxa are higher (red) or lower (blue) in each group.

1367

1368

1369

1370

1371

1372

1373

1374

1375

1376

Figure S9: Graphical summary of LEfSe analysis from the dissected tissues of *Am. maculatum.* A) *R. parkeri*-infected and uninfected and B) unfed and partially fed *Am. maculatum.* Significant taxa are ranked in decreasing order by their LDA scores (x axis). The mini heat map to the right of the plot indicates whether the number of taxa are higher (red) or lower (blue) in each group.
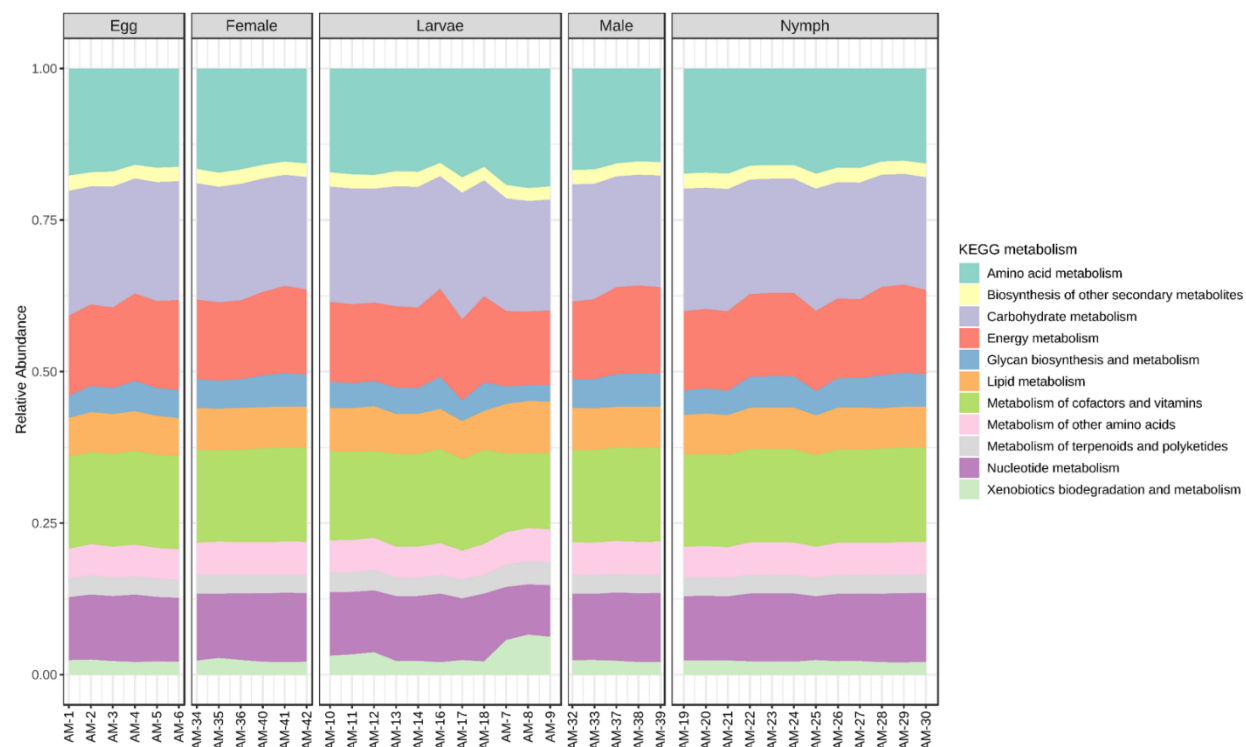
1377

Figure S10: Histogram indicating functional differences of the *Am. maculatum* microbiota across developmental stages. KEGG metabolic categories were obtained from 16S rRNA gene sequences using the PICRUSt2 pipeline.
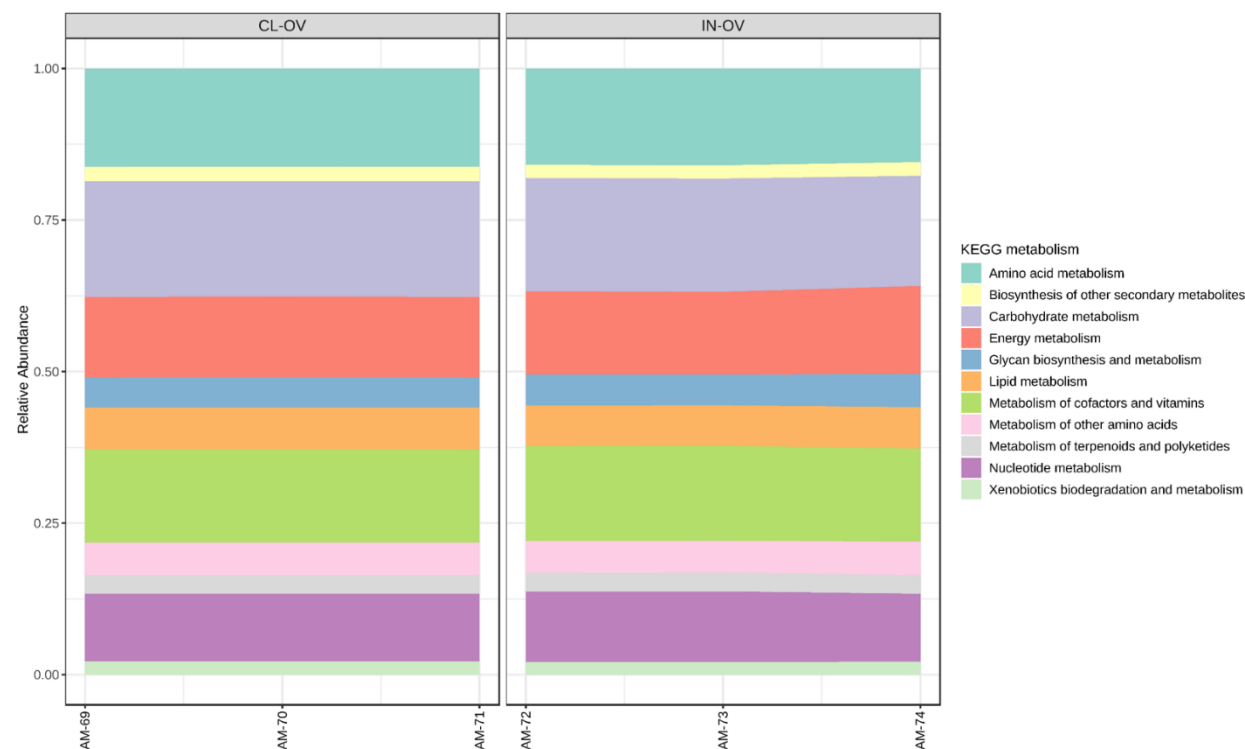
1378

1379

1380

1381

Figure S11: Histogram indicating functional differences in the ovaries of the *Am. maculatum* microbiota with and without *R. parkeri* infection. KEGG metabolic categories were obtained from 16S rRNA gene sequences using the PICRUSt2 pipeline.

1382

1383

1384 **Additional Table**

Table S1: Demultiplexed sequence counts summary

	Forward reads	Reverse reads
Mean	45453.5	45453.5
Maximum	112242	112242
Total	4090811	4090811

1385